Viral proteins as novel therapeutics in chronic horse wounds

Kirsty Anne Wakelin

A thesis submitted in partial fulfilment of the Bachelor of Biomedical Science with Honours

Department of Microbiology and Immunology

University of Otago

Dunedin, New Zealand

October, 2015

Abstract

Skin wounds are a prevalent problem for the equine industry, both for the well-being of the animals and the financial impact of treatment. Chronic wounds often arise in horses, and this is thought to be due to poor vascularisation, sustained inflammation and high tissue tension preventing the wound from closing efficiently. Chronic wounds can take months to heal and can increase the risk of secondary infections.

Previous research has identified two Orf virus proteins, VEGF-E and viral (v)IL-10, which decreased the immune response and improved healing in murine models of burn and traumatic wounds. Orf virus IL-10 is an anti-inflammatory cytokine that reduces inflammatory signalling and macrophage infiltration, thereby reducing fibrosis and scarring. VEGF-E is a vascular endothelial growth factor that promotes wound re-epithelialisation, re-vascularisation and closure. As these proteins work across a range of species, it was hypothesised that similar effects would be seen if these proteins were administered to chronic wounds in horses. The aims of this research project were to assess if the two viral proteins' functions extended to equine cells and tissues.

An equine cell line was generated by culturing cells from a thoroughbred horse skin biopsy. Cell proliferation and migration in the presence of the viral proteins was examined using a wound scratch assay. No changes in closure rate were observed after incubation with either protein. RNA expression in response to the viral proteins in the presence and absence of inflammatory stimuli was examined using quantitative PCR. Changes in inflammatory and fibrosis gene expression were observed in response to vIL-10.

Biopsies from chronic equine wounds, with or without VEGF-E and vIL-10 treatment, were analysed for regulatory and histological changes. Quantitative PCR

analysis of wound biopsies taken after 2, 7 and 14 days, and after final wound closure, showed an immediate reduction in some inflammatory and fibrotic mediators in treated wounds. Histological analysis showed a temporary increase in the thickness and length of the regenerating epidermis in treated skin. Immunohistochemical analysis of wound sections showed increased angiogenesis in the newly forming granulation tissue in treated skin, and a reduction in the infiltration of innate immune cells.

These findings suggest that the viral proteins are active on equine cells but that the dosage and timing for treatments with VEGF-E and vIL-10 require optimisation to gain therapeutic benefits.

Acknowledgements

Firstly, I would like to extend a huge thank you to my supervisor, Dr Lyn Wise, for all the support and encouragement this year. I greatly appreciate all your patience with me, and the wealth of knowledge and advice that you have imparted on me throughout the year.

I would also like to thank Gabs and Nicky, for all your help in the lab. You have taught me so many valuable skills and have made my year so much more enjoyable with your happy, helpful attitudes. It demonstrates how much I fully appreciate all your hard work that I have not filed a single hurt feelings report this year.

Thank you to the VRU students for keeping me sane when it all started to get a bit much, and for making the lab and write-up room a place that I looked forward to coming to every day. Thank you also to Andy, Steve and Ells, for making me feel so welcome in the VRU team. I have loved every minute of it.

A huge thank you to my parents. I could not have done this without all your support, phone calls and wonderful care packages. Thank you to my friends, especially my flatmates who have endured enough whinging and crying to last them a lifetime.

And finally, to Ryan. There is no way I could have done any of this without your constant support and encouragement. Thank you doesn't begin to cover it.

Table of Contents

Table of Figures

Table of Tables

List of Abbreviations

BSA	Bovine Serum Albumin
CA	Carbonic Anhydrase
cDNA	Complementary DNA
DAPI	4’6-diamino-2-phenylindole
DMEM	Dulbecco’s Modified Eagle’s Medium
DMSO	Dimethyl Sulfoxide
eFAM	Equine Fibroblast Assay Medium
eFGM	Equine Fibroblast Growth Medium
eKGM	Equine Keratinocyte Growth Medium
EGF	Epidermal Growth Factor
EGT	Exuberant Granulation Tissue
EMEM	Eagle’s Minimum Essential Medium
FCS	Fetal Calf Serum
FGF	Fibroblast Growth Factor
GAPDH	Glyceraldehyde-3-phosphate Dehydrogenase
HGF	Hepatocyte Growth Factor
IL	Interleukin
IV	Intravenous
MHC	Major Histocompatibility Complex
MMP	Matrix Metalloproteinase
MSB	Martius Scarlet Blue
MW	Molecular Weight
OV	Orf Virus
PBS	Phopshate-Buffered Saline
PCR	Polymerase Chain Reaction
PDGF	Platelet-Derived Growth Factor
PolyI:C	Polyinosinic:polycytidylic acid
PSK	Penicillin, Streptomycin & Kanamycin
SMA	Smooth Muscle Actin
TAE	Tris Acetic Acid
TBS	Tris-Buffered Saline

TGF	Transforming Growth Factor
UV	Ultraviolet
VEGF	Vascular Endothelial Growth Factor
Vim	Vimentin
vWF	von-Willebrand Factor

1 Introduction

1.1 Structure of skin

Skin is the outermost barrier for the body, which protects the internal organs from external insults and water loss. It is a highly regenerative, complex tissue that is made up of two main layers; the outer epidermis and the underlying dermis. The epidermis consists of a stratified epithelium made up of approximately 95% keratinocytes (Lai-Cheong and McGrath, 2009). The basal keratinocytes are highly proliferative and produce daughter cells, which differentiate through the five layers of the epidermis: the strata basale, spinous, granular, lucid (found only in thick areas such as soles of feet and palms of hands) and the outermost stratum corneum. (Lai-Cheong and McGrath, 2009; Wickett and Visscher, 2006). The stratum corneum is highly stratified and the keratinocytes in this layer undergo nuclear digestion and envelope cross-linking to differentiate into corneocytes. They are constantly shed to protect the skin from absorption of chemicals and infection by pathogens. The other 5% of cells in the epidermis are the melanocytes which provide the skin with pigment, Merkel cells which transmit sensory information, and Langerhan cells (dendritic immune cells) which clear pathogens by phagocytosis (Lai-Cheong and McGrath, 2009).

The epidermis is separated from the underlying dermis via a thin basement membrane, consisting of less than 200 nm of closely intertwined proteins which link the basal keratinocytes to the fibres of collagen within the dermis (Lai-Cheong and McGrath, 2009). The underlying dermal layer is subdivided into two parts: the papillary dermis and reticular dermis. The papillary dermis is in contact with the basement membrane and contains blood vessels and sensory nerve endings. The reticular dermis sits deeper than the papillary dermis and functions to attach the entire dermis to the

subcutis layer (Lai-Cheong and McGrath, 2009). The dermis is also rich with connective tissue, and the cells that produce this matrix, fibroblasts. The dermis also contains mast cells and specialised macrophages to aid in immune control and clearance of unwanted debris (Yung, 2014). Other skin components, such as hair follicles and glands, are rooted in the dermal layer and project up through the epidermis (Martin, 1997).

1.2 Stages of wound healing

When skin is wounded, a series of events occur to allow the skin to regenerate and heal over time. These can be divided into three major stages: inflammation, repair and remodelling (Gurtner *et al.*, 2008). Inflammation is the first stage of wound healing and is characterised by haemostasis, which stops bleeding, followed by an infiltration of immune cells into the wound bed. Haemostasis is induced by platelet aggregation and clotting factors to form a fibrin clot. This clot plugs the damaged blood vessels and creates a matrix onto which the incoming inflammatory cells and growth factors can attach.

The neutrophils and macrophages play an important role in initial wound healing and arrive sequentially after wounding. They enter the surrounding tissues through damaged blood vessels, and are attracted to the site of injury by chemokines, such as momcyte chemotactic protein (MCP-1) and macrophage inflammatory protein (MIP-2α) produced by activated immune cells that are already present in the injured tissue (Shaw and Martin, 2009). Neutrophil invasion generally clears after a few days, while macrophages continue to accumulate to assist in wound healing (Martin, 1997). These immune cells are important in the onset of fibrosis and the debridement of the wound (Leibovich and Ross, 1975; Wynn and Barron, 2010).

Aggregated platelets and activated innate immune cells produce growth factors such as vascular endothelial growth factor (VEGF), platelet-derived growth factor (PDGF), epidermal growth factor (EGF) and transforming growth factor (TGFβ). These growth factors play an important part in immediate wound healing by encouraging epithelial cell migration, upregulation of fibrotic genes in fibroblasts, and vascularisation (Barrientos *et al*., 2008; Martin, 1997).

After haemostasis has been achieved and inflammatory cells have phagocytosed any foreign pathogens, the next step in wound repair is re-epithelialisation. At this point, activated macrophages produce cytokines such as interleukin (IL)-10 and transforming growth factor ($TGF\beta_1$), which dampen down the immune response and inhibit further inflammation (Wynn and Barron, 2010).

Re-epithelialisation occurs two to ten days after the initial injury and during this phase, the basal keratinocytes in the epidermis migrate across the wounded space in response to stimuli such as EGF and VEGF (Barrientos *et al*., 2008). In order to do this, keratinocytes need to free themselves from the basal membrane by dissolving hemidesmosome integrin attachments from the basal laminin. The keratinocytes closest to the wound edge then express new integrins that allow them to migrate along the basal lamina. In order to migrate through the fibrin clot, these cells must express plasmin and matrix metalloproteinases (MMPs) to dissolve the fibrin and collagen network (Martin, 1997). The integrin expression is restored to allow the basal keratinocytes to cease migration and anchor to the basement membrane.

Fibroblasts migrate into the lower wound space from the dermis and lay down a disorganised matrix of collagen (Gurtner *et al*., 2008). The underlying connective tissue laid down by fibroblasts begins to contract to bring the wound margins in closer and aid the rate of re-epithelialisation. This contraction is largely due to the activity of

myofibroblasts, a specialised differentiation of fibroblasts with contractile muscle actin (Gurtner *et al*., 2008). The new collagen matrix aids vascularisation, which aims to supply the new tissue with an adequate blood circulation (Gurtner *et al*., 2008). An important growth factor that contributes to the formation of new blood vessels during tissue repair is vascular endothelial growth factor (VEGF)-A (Galiano *et al*., 2004; Gurtner *et al.*, 2008; Johnson and Wilgus, 2014). This class of growth factors act through the specific receptors VEGF Receptor (VEGFR)-1, VEGFR-2 and VEGFR-3 (Johnson and Wilgus, 2014). VEGF-A only binds to VEGFR-1 and VEGFR-2 (Holmes *et al*., 2007). VEGFR-2 has been shown to promote cellular migration and proliferation, and is mostly expressed on vascular endothelial cells to increase vascularisation (Holmes *et al*., 2007). VEGFR-1 has a higher affinity for VEGF-A than VEGFR-2, and is expressed on vascular endothelial cells. This receptor is also expressed on macrophages to promote inflammation and has been implicated in inflammatory diseases (Shibuya, 2006). VEGF-A can act through both receptors to increase angiogenesis and inflammation during the repair stage of wound healing (Johnson and Wilgus, 2014).

The final step of wound healing is resolution, which is important in restoring functionality to the skin and preventing scarring. Once the keratinocytes have migrated across the entire surface of the wound they restore hemidesmosome attachments and differentiate to regenerate the stratified epithelium (Shaw and Martin, 2009). If the wound penetrates into the dermis, sweat glands and hair follicles may be destroyed. The regenerating skin cells are unable to create new hair or sweat glands and hence the resolved wound would lack these appendages (Martin, 1997).

New blood vessels form rapidly during angiogenesis and undergo maturation to create a refined and functional vascular network (Shaw and Martin, 2009). In the

dermal scar, MMPs such as collagenase-1 are produced to degrade the collagen III matrix and slowly replace it with collagen I. This remodelling helps to strengthen the new tissue to prevent further damage and restore the protective function of the skin. During this resolution stage there is programmed cell death of many of the contractile myofibroblasts, endothelial cells and macrophages, which leaves an acellular scar (Gurtner *et al*., 2008).

1.3 Pathologies associated with wound healing

The process of wound healing is usually a tightly controlled process that successfully restores the skin's protective function. However, this process is not always a flawless mechanism, and can often fail to heal correctly in individuals with underlying health concerns or those with genetic abnormalities (Sen *et al*., 2009). Incorrect healing can lead to numerous pathologies, the extremes of which are chronic wounds or fibroproliferative scars.

Chronic wounds are persistent, non-healing wounds, which fail to close in a timely fashion and pose a high risk for secondary infections. Chronic wounds often feature prolonged inflammation and a reduction in epithelial regeneration (Demidova-Rice *et al*., 2012). A main subset of human chronic wounds is vascular ulcers, which can be a result of limited blood supply due to arterial blockages (arterial ulcers) or a rise in venous pressure causing a back-flow of venous blood (venous ulcers). Both forms of chronic wounds, along with wounds associated with diabetes or neuropathies, fail to heal and as a result they are able to develop secondary infections that pose a serious risk of blood-borne disease to the patient (Demidova-Rice *et al*., 2012).

In humans, fibroproliferative scars are called keloids which are the result of fibroblasts laying down too much fibrin and collagen rapidly, preventing the growth of epithelial cells. This over-activity of fibroblasts is uncommon across most mammalian

species and is almost completely limited to humans and horses (Ud-Din *et al*., 2014). The predisposition to form keloids in humans has been linked to differences in gene expression between normal fibroblasts and those isolated from keloid scars (Russell *et al*., 2010).

Wound healing pathologies are significant due to the large impact they have on the health system and economy. Wound pathologies are fairly common, as they can arise from a variety of causes and affect more than 6 million patients a year in the United States alone (Sen *et al*., 2009). The economic burden of wounds is rising every year due to an increase in other health-related issues such as diabetes and obesity. As a result the current market cannot provide adequate treatments to keep up with the demand (Sen *et al*., 2009).

1.4 Biological wound therapies

Biological therapies by definition are a broad range of therapies that target wound healing by promoting stimulation of the body's own healing responses (Braddock *et al*., 1999; Rennert *et al*., 2013). Such therapies are designed to target processes that are altered in certain diseased states in order to restore effective wound healing. Today there are many products that aid in the resolution of chronic wounds, including biological skin equivalents, growth factors and stem cell therapies (Braddock *et al*., 1999; Brown *et al*., 1989; Rennert *et al*., 2013).

Chronic wounds are thought to be caused by a dysregulation of endogenous growth factors. An increasing area of interest for biological wound therapies involves the application of exogenous growth factors (Rennert *et al*., 2013). Many growth factors, such as PDGF, $TGF\beta_1$, EGF and VEGF-A have previously been shown to improve the rate of wound repair in chronic wounds (Beck *et al*., 1991; Brown *et al*., 1989; Heldin and Westermark, 1999; Nall *et al*., 1996).

Biological skin equivalents are also highly common forms of treatment for chronic wounds, and these are composed of a complex of cells and matrix proteins that are placed over the wound area to promote wound re-epithelisation and repair (Rennert *et al*., 2013).

Keloid scars require a different approach for therapies than chronic wounds as they result from over proliferation. The underlying cause of keloid scars is somewhat unclear, but there is a lot of research into potential treatments (Viera *et al*., 2010). Growth factors are also important for treatments against hypertrophic scars. Hepatocyte growth factor (HGF) is involved in angiogenesis, which increases the blood supply to the granulation tissue of the wound. This growth factor also alters levels of cytokines such as TGFβ1, which have been implicated in the formation of hypertrophic scars (Ono *et al*., 2004). Basic fibroblast growth factor (FGF-2) helps inhibit the production of excess collagen in fibrosis and assists in increasing the rate of wound closure (Ono *et al*., 2007). While these growth factors aid in reducing the production of hypertrophic scars, other treatments can also contribute to the process. Treatments include neutralising antibodies or small interfering RNAs against growth factors such as TGFs, which are involved in cell proliferation and collagen production. As mentioned above, other growth factors like HGF are also used to target the detrimental effects of these growth factors (Viera *et al*., 2010).

1.5 Wound healing processes and treatments in horses

Problematic wounds in humans are challenging to understand and appropriate animal models would help to gain a better idea of the underlying problems in aberrant wound healing processes. The solution may lie in veterinary medicine, as a number of human complications are found in companion animals such as horses (Theoret and Wilmink, 2013; Volk and Bohling, 2013).

Horses are prone to developing traumatic injuries in the limb due to their tendency to flee during the fight or flight response. These wounds usually result in large areas of tissue loss and as a result are left to heal by second intention (left open to heal with no suturing), which can often take a long time to heal (Theoret and Wilmink, 2013). While body wounds usually heal with no detrimental effects after 4 weeks, limb wounds often take 10 to 12 weeks to heal. This can lead to the development of chronic wounds or excessive fibrosis.

Horses, like humans, develop chronic wounds that fail to close and pose risks for further infection (Westgate *et al*., 2010). The tendency to form chronic wounds is thought to stem from the high tissue tension in limbs, as well as a poor vascular supply and constant contamination of the wound (Westgate *et al*., 2010). Studies have shown that contraction is a key mediator in second intention wound healing, which is controlled by differentiated myofibroblasts that contain actin filaments (Wilmink and van Weeren, 2004). The myofibroblasts in horses are less organised compared to pony wounds, which results in a slower rate of contraction (Wilmink *et al*., 1999b). Epithelialisation of horse limb wounds starts much later in the wound healing time course (after 4 weeks compared to 3 weeks in muscle wounds). This delayed epithelialisation and lack of wound contraction aid in the formation of chronic wounds (Wilmink *et al*., 1999a). The inflammatory response in horses has also shown to be implicated in the slow rate of healing of limb wounds (van den Boom *et al*., 2002; Wilmink *et al*., 1999b). Inflammatory cells reside in limb wounds longer than in body wounds, and an extended inflammatory response may be preventing the onset of fibrosis to allow the wound to heal (Wilmink *et al*., 1999b). Fibrin deposits in the limb wounds fail to clear effectively after the initial inflammation stage, which can hinder re-epithelialisation. This is another indication that the inflammatory response is

dysregulated in limb wounds of horses, causing the formation of chronic, non–healing wounds.

Horses can also develop fibrotic wounds called exuberant granulation tissue (EGT), not unlike keloid scars in humans (Theoret and Wilmink, 2013). It has been reported that horses also have a genetic predisposition to forming EGT which contain a unique subset of fibroblasts (Theoret *et al*., 2013). The process of bandaging the limbs may extrapolate the formation of EGT, or "proud flesh". These EGT scars are detrimental to limb function and are susceptible to re-injury. The etiology and formation of these scars are very similar in humans and horses, the only difference being that EGT is not epithelialised (Theoret and Wilmink, 2013). EGT formation is due to an excessive rate of fibrosis that grows over the margins of the wound area. $TGF\beta_1$ has been implicated in the formation of EGT in the limbs of horses. Levels of $TGF\beta_1$ are elevated in limb wounds compared to body wounds and this pro-fibrotic cytokine can increase the production of collagens to promote the onset of EGT (Theoret *et al*., 2001; van den Boom *et al*., 2002). EGT is often characterised by an increase in the production of new blood vessels (angiogenesis) (Dubuc *et al*., 2006; Lepault *et al*., 2005). However, these vessels are often occluded and so lack the capacity to supply blood to the tissue. This generates a hypoxic environment that promotes the excessive production of extracellular matrix, resulting in formation of EGT.

Many studies have looked at the effects of human therapies on equine wounds, such as topical treatments and debridement and several studies have investigated genes involved in the production of exuberant granulation tissue in an attempt to identify a therapeutic target (Berry and Sullins, 2003; Sherman *et al*., 2007). Topical treatments are commonly used in both human and animal practice and involve applying a substance to the wound followed by bandaging/strapping the wound to prevent the

treatment from shifting. The downside to this sort of treatment is the requirement of bandaging, which as mentioned above has been shown to encourage the development of EGT (Theoret *et al*., 2002). Treating these equine wounds is challenging, as horses are highly active and limb immobilisation is not possible.

A common type of equine wound therapy is the application of antimicrobial compounds such as povidine (iodine) ointment, manuka honey, bacitracin or silver sulfadiazine (Berry and Sullins, 2003; Bischofberger *et al*., 2011; Engelen *et al*., 2004). Antimicrobials are thought to aid in wound healing by clearing infection, as this bacterial colonisation has been implicated as a cause of chronic wounds (Westgate *et al*., 2010). These topical treatments are able to prevent secondary infections from occurring, but used alone they fail to improve the rate of wound closure (Berry and Sullins, 2003; Bischofberger *et al*., 2011).

As well as antimicrobial therapies, many studies have looked at the effect of alternative human therapies such as maggot debridement, topical oxygen therapy and stem cell therapies (Bussche *et al*., 2015; Sherman *et al*., 2007; Theoret, 2009; Tracey *et al*., 2014). This class of treatments aim to improve the wound microenvironment to allow optimal healing. However, they are often difficult to administer and require multiple treatment sessions, which puts physical and financial strain on owners.

The use of biological therapies has been well-researched in human wounds, and involves the addition of biological factors such as connective tissue components or growth factors to the wound site. Some examples of biological therapies studied in horses include ketanserin, bovine collagen and activated protein C (Bello, 2002; Bischofberger *et al*., 2015; Engelen *et al*., 2004). These treatments aim to target components of wound healing that have been shown to be altered in pathologies such as chronic wounds or EGT, such as irregular inflammation and fibrosis. Biological

therapies reduce the requirement for surgeries or bandaging, to reduce time, money and stress on the animal.

Cytokines and growth factors are also being investigated for the treatment of both chronic and fibrotic wounds in humans, yet very little research has been undertaken in horses. It is likely that new protein therapies can be developed to target the healing impairments associated with equine wounds. Evaluation of these protein therapies in equine wounds would also provide valuable information regarding their potential use in similar human conditions.

1.6 Orf virus and wound healing

Orf virus (OV) is part of the parapoxvirus genus and has the ability to cause pustular and exanthemous lesions in sheep, goats and humans. OV infection initiates in wounded skin and lesions formed by the virus are highly vascularised and proliferative. However, these lesions heal successfully with limited scarring. Investigation into the genome of the virus identified a set of host manipulating factors, of which two proteins were identified as a potential cause of the successful resolution: vascular endothelial growth factor (VEGF)-E, a homolog of human VEGF, and OV interleukin-10 (vIL-10), an anti-inflammatory cytokine. The cellular homologs of these factors (VEGF-A and IL-10) are key mediators in the regulation and maintenance of the wound healing response. Viral versions of these genes have demonstrated enhanced wound healing capabilities in smaller mammals such as mice (Fleming *et al*., 2015; Mercer *et al*., 2006; Wise *et al*., 2012; Wise *et al*., 2014).

As described previously in this report, cellular VEGF-A aids in the deposition of the fibrin matrix and induces blood vessel and epidermal regeneration, which it performs through the interaction with VEGFR2 (Johnson and Wilgus, 2014; Wise *et al*., 2012). VEGF-A also binds to VEGFR1 and this activity can lead to sustained

vascular leakage and tissue inflammation. VEGF-E binds solely to VEGFR2 and due to this specific interaction it does not have the adverse inflammatory effects caused by VEGF-A (Wise *et al*., 1999). The VEGF-E homolog was shown to induce vascularisation in mice, as well as an increase in epidermal thickness and wound re-epithelialisation (Wise *et al*., 2012). The activation of keratinocytes and endothelial cells without the increased inflammation allows VEGF-E to improve wound closure and resolution, making this an ideal candidate for treatment of chronic wounds in horses.

OV produces a second protein, vIL-10, which helps wound resolution (Wise *et al*., 2014). Mammalian IL-10 is an anti-inflammatory cytokine that helps to limit inflammation by preventing the infiltration of macrophages and neutrophils to the wound site (Sato *et al*., 1999). It has also been implicated in control of scar tissue formation. This viral homolog of IL-10 was shown to exhibit similar effects in that it limited macrophage infiltration and reduced the expression of key inflammatory genes. It also accelerated wound re-epithelialisation and reduced fibrosis and scar tissue formation (Wise *et al*., 2014).

Combining the viral VEGF-E with the viral IL-10 demonstrated a greater improvement in wound healing, and further reduced inflammation and fibrosis (unpublished data). These observations were not seen in wounds treated with the equivalent cellular combination (VEGF-A and IL-10). The viral proteins have been shown to be active across a range of species, including ovine, murine, human, bovine and ovine (Wise *et al*., 2007; Wise *et al*., 2012; Wise *et al*., 2014; Wise *et al*., 2003; Wise *et al*., 1999), and there is a high level of homology between the protein receptors across these species (84 – 98% for VEGF-E, 53 – 93% for vIL-10), hence it is likely that the proteins will also be active in equine species.

1.7 Hypothesis and aims

The specific activities of VEGF-E and viral IL-10 led to the hypothesis that a combination treatment will promote closure and limit EGT formation in equine limb wounds. Specifically, the proteins will achieve this by promoting wound re-epithelialisation and re-vascularisation while limiting inflammation and fibrosis in equine wounds. The aim of this project is to determine if the viral proteins are biologically active in equine cells and tissues. This aim will be approached by two studies; *in vitro* in an equine cell line to determine if the proteins are active in these cells and *in vivo* in chronic wounds of thoroughbred horses to determine if the proteins are able to improve wound re-epithelialisation and re-vascularisation, and limit wound inflammation.

2 Materials and Methods

2.1 Protein methods

2.1.1 Protein production

HEK293-EBNA cells transfected with a plasmid encoding FLAG-tagged versions of the VEGF-E or vIL-10 genes were used for protein production (Imlach *et al*., 2002; Wise *et al*., 2003). The cells were grown in Dulbecco's Modified Eagle's Medium (DMEM) containing 10% heat-inactivated fetal calf serum (FCS), 50 ng/mL gentamicin, 2 unit/mL penicillin, 1 µg/mL streptomycin and 0.2 µg/mL kanamycin (PSK) and 20 mg/mL hygromycin B (Sigma). Cells were grown at 37 ^{o}C in 5% CO_2 until confluent, then the supernatant was collected, clarified by centrifugation at 1,200 rpm for 5 min, then stored at -80 °C.

2.1.2 Protein purification and concentration

Supernatant containing FLAG-tagged protein was transferred to 200 mL disposable centrifugation tubes with 200 µL of M2 anti-FLAG agarose beads (Sigma). Tubes were rotated overnight at 4 °C then beads were separated from the supernatant using a chromatography column. The beads were then washed three times with 10 mL tris-buffered saline containing 0.02% Tween-20 (TBS-T). FLAG peptide (Sigma) was then added to the column at a concentration of 100 µg in 5 mL volume of TBS-T and the eluted protein was collected. The thawed protein was concentrated, and residual FLAG peptide removed using a filtered centrifuge tube (Amicon Ultra15, 15kDa pore size) spun at 5,000 rpm for 30 min at 4 °C. The protein was then buffer exchanged by the addition of 5 mL filter-sterilised phosphate-buffered saline (PBS), which was reduced to a final volume of 500 µL by centrifugation as described above. The final protein stock was distributed into aliquots and stored at -80 °C.

2.1.3 Protein concentration and quantification

Protein samples were diluted 1:1 with reducing sample buffer then boiled for 5 min. Full-range rainbow marker (5 µL, Amersham, RPN800E), 3 µL, 8 µL and 20 µL of carbonic anhydrase (CA), purified VEGF-E and vIL-10 were loaded into wells. The proteins were resolved on a 10-15% stacked SDS-page gel run at 100 V for 2 hr. Gels were then stained overnight with Coomassie blue, destained in methanol and photographed using the BioRad ChemiDoc. Band densities were measured using ImageJ software and the readings for CA were used to generate a standard curve. Concentrations of purified VEGF-E and vIL-10 were calculated by taking the average of the three band densities and using the equation from the standard curve.

2.2 Equine cell culture and characterisation

2.2.1 Trypsin cell extraction

Equine skin samples were obtained from a trial conducted at Massey University with Institutional approval (MUAEC 14/84). Cells were extracted from equine skin using a method adapted from Yamada (Yamada, 2003). Biopsies (four x 25 mm^2) of equine skin from the thoracic (body) and metacarpal (limb) regions were sanitised by soaking in Betadine for three periods of 1 minute, followed by incubation in 0.25% trypsin overnight at 4 °C. The epidermis was then scraped from the dermis using sterile forceps and a scalpel, and each was then processed through a cell strainer to separate the cells. The body and limb cell suspensions were resuspended in 5 mL equine fibroblast growth media (eFGM): DMEM supplemented with 10% FCS, 50 ng/mL gentamicin, PSK (concentrations indicated in 2.1.1) and 29 µg/mL L-glutamine, or in 5 mL equine keratinocyte growth media (eKGM): Eagle's Minimum Essential Medium (EMEM) supplemented with 10% FCS with Ca^{2+} chelated with 50 mg/mL Chelex 100 Resin (Bio Rad, 1421253), 50 ng/mL gentamicin, PSK (concentrations indicated in

2.1.1) and 29 μg/mL L-glutamine. Cells were incubated in a 96-well plate at 37 °C in 5% CO_2 until colonies were obtained. Wells containing single colonies were harvested using 25 mg/mL trypsin, counted using trypan blue exclusion on a haemocytometer, and were maintained at a density of between 1 x 10^4 – 1 x 10^5 cells/mL. Once the fibroblast lines were created, aliquots of 1 x 10^7 cells were diluted in 1 mL 10% DMSO/80% DMEM/10% FCS and were placed in liquid nitrogen storage.

2.2.2 Collagenase dispase cell extraction

Cells were extracted from equine skin using Collagenase/Dispase digestion following the manufacturer's instructions. Biopsies (four x 25 mm^2) of body and limb equine skin were sanitised by soaking in Betadine for three periods of 1 minute and were incubated in 100 mg/mL Collagenase/Dispase (Roche) in PBS overnight at 4 °C. The skin was processed through a metal tea strainer to remove debris, followed by a cell strainer to separate the cells. The body and limb cell suspensions were resuspended in 5 mL eFGM or in 5 mL eKGM. Cells were incubated in a 96-well plate at 37 ^oC in 5% CO_2 until colonies were obtained. Wells containing single colonies were harvested using 25 mg/mL trypsin, counted using trypan blue exclusion on a haemocytometer, and were maintained at a density of between 1 x 10^4 – 1 x 10^5 cells/mL. Once the fibroblast lines were created, aliquots of 1 x 10^7 cells were diluted in 1 mL 10% DMSO/80% DMEM/10% FCS and were placed in liquid nitrogen storage.

2.2.3 Explant cell extraction

Cells were extracted from equine skin using a method that was adapted from Vangipuram *et al.* (Vangipuram *et al.*, 2013). Tissue culture plates (6-well) were coated in filter-sterilised 0.1% gelatin in PBS for 30 min, after which the gelatin was removed. Biopsies (four x 25 mm^2) of body and limb equine skin were dissected to 1 mm^2 explants and three were placed on the gelatin coating in each well. Following 7 day

incubation in 0.4 mL eFGM, explants were removed and the medium was replaced with either eFGM or eKGM. Wells containing large colonies were harvested using 25 mg/mL trypsin, counted using trypan blue exclusion on a haemocytometer, and were maintained at a density of between 1 x 10^4 – 1 x 10^5 cells/mL. Once the fibroblast lines were created, aliquots of 1 x 10^7 cells were diluted in 1 mL 10% DMSO/80% DMEM/10% FCS then were placed in liquid nitrogen storage.

2.2.4 Immunofluorescent analysis of equine fibroblasts

Equine fibroblasts ($5x10^5$) were seeded into a 6-well plate containing sterilised 4 cm^2 coverslips and incubated in eFGM at 37 °C in 5% CO_2 until confluent. Media was removed from the wells and cells were fixed overnight in 0.5% Zinc-Salts fixative. Cells were then equilibrated in TBS for 20 min and incubated with antibodies against vimentin (Vim, Cell Signaling Technology; 1:50 dilution) and α-smooth muscle actin (αSMA, Sigma-Aldrich; 1:400 dilution) in 20 µL of TBS containing 0.1% bovine serum albumin for 2 h at room temperature. For the final 30 min of the incubation, 20 µL of 4',6-diamidino-2-phenylindole (DAPI, 75 nM, Invitrogen) was added, followed by a TBS wash. Coverslips were mounted onto microscope slides using SlowFade Gold (7 µL, Invitrogen) and stored at 4 °C overnight. Stained cells were photographed at 40 X magnification on the upright fluorescence microscope (Olympus BX-51) using cellSens Software (Olympus). Images were prepared on Adobe Photoshop.

2.2.5 PCR analysis of fibroblast receptors

Equine fibroblasts (3 x 10^6) were grown to confluence in a 75 cm^2 tissue culture flask. Cells were washed with PBS and harvested using 0.25% trypsin, and pelleted by centrifugation at 1,200 rpm. Cells were then homogenised in lysis buffer (Qiagen) using a 1 mL syringe and a 20-gauge needle. RNA was isolated using the Geneaid TriRNA Pure Kit according to the manufacturer's instructions. Quanta Biosciences'

PerfeCta DNase I (RNase-free) was used following the manufacturer's instructions to remove DNA contamination, and sample concentrations (ng/μL), 260/230 and 260/280 ratios were determined with a spectrophotometer (NanoDrop). Synthesis of cDNA was carried out with SuperScript III First-Strand Synthesis SuperMix for qRT-PCR (Invitrogen) following the manufacturer's instructions, using 500 ng RNA/rxn.

A standard PCR reaction was carried out using the Expand High Fidelity PCR System (Roche) in a 50μL volume. Forward and reverse primers used to detect equine VEGFR1, VEGFR2 and IL-10Rα genes are listed in Appendix 1, Supplementary Table 1. Each reaction mix contained 5% of the cDNA sample and 100 mM of each primer and underwent the following cycling protocol: denaturation at 94 °C for 15 sec, annealing at 60 °C for 30 sec and elongation at 72 °C for 45 seconds. The PCR products were analysed on a 1% agarose gel containing 500 ng/mL ethidium bromide. DNA ladder (3.5 μl of 1Kb Plus, Invitrogen) or 10 μl of PCR product was added to each well in loading dye. Gel electrophoresis was conducted in TAE buffer at 100V for 1 h. Bands were visualised under UV light using Chemi-Doc XRS using the Quantity One software (Bio-Rad).

2.3 Assays with equine fibroblasts

2.3.1 Quantitative PCR analysis of gene expression

Changes in gene expression in response to the proteins were assessed using quantitative PCR. Equine fibroblasts (3 x 10^6) were seeded in 75 cm^2 tissue culture flasks and grown to confluence in 10 mL eFGM. Media was removed and cells were washed twice in PBS before the addition of 10 mL DMEM supplemented with 0.1% BSA, 50 ng/mL gentamicin, PSK (concentrations indicated in 2.1.1) and 29 μg/mL L-glutamine (equine fibroblast assay medium, eFAM). To promote quiescence, cells were incubated in this basal media overnight at 37 °C in 5% CO_2. Cells were washed in PBS

twice and 10 mL of eFAM containing 200 ng/mL VEGF-E or 20 ng/mL vIL-10 or media alone was added. An additional set of flasks were treated with the above and 50 μg/mL polyinosinic:polycytidylic acid (PolyI:C) to induce an inflammatory response in the cells. The fibroblasts were incubated for 2 h then washed twice with PBS and harvested using 0.25% trypsin. eFGM was added to neutralise the trypsin and cells were spun down in a microcentrifuge at 1,200 rpm to form a pellet. Cells were homogenised and lysed to extract RNA, followed by cDNA synthesis as per section 2.2.5.

Quantitative PCRs were conducted using cDNA equivalent of 5ng RNA, the SYBR GreenER qPCR SuperMix (Invitrogen) and the Applied Biosystems 7500 Fast PCR machine, using primers in Appendix 1, Supplementary Table 1. Primer efficiencies were calculated and expression levels of genes were determined relative to glyceraldehyde-3-phosphate dehydrogenase (GAPDH) and to the levels in cells treated with media only.

2.3.2 *In vitro* cellular migration assay

Equine fibroblasts (1.25×10^5) were seeded into a 24-well plate and grown to confluence in eFGM. Wells with confluent monolayers of cells were scratched down the centre of the well with a 200 μL pipette tip following a protocol adapted from Hulkower (Hulkower and Herber, 2011). Media and damaged cells were removed, and wells were washed twice with PBS. In initial assays, the media was replaced with 1 mL of eFAM containing 0-2% FCS or 0.1% BSA. In subsequent assays, the media was replaced with 1mL of either 200 ng/mL VEGF-E or 20 ng/mL vIL-10 in eFAM containing 0.1% BSA, or with media alone. Three replicate images were taken at the centre of each scratch at 0, 6, 12, 24 and 48 hours at 20 X magnification using the Olympus TH4-200 inverted microscope and the cellSens Software. In each image the

scratch area was measured using ImageJ. Changes in the scratch area were calculated as ratio of the original area at time = 0 h using the following equation:

$$Ratio\ of\ original\ scratch\ of\ closure = \left(\frac{Scratch\ area\ at\ time\ (t)}{Original\ scratch\ area\ (t=0)}\right)$$

2.4 Equine skin methods

2.4.1 Equine wound trial

A trial was undertaken in thoroughbred horses to assess the effects of viral treatment in equine skin wounds. The trial was conducted at Massey University by Christine Theoret, Chris Riley and Christa Bodaan, with Institutional approval (MUAEC 14/84). Four horses were assigned to the chronic wound group. These horses were sedated with detomidine hydrochloride (0.01 mg/kg; intravenous (IV)) and butorphanol tartrate (0.04 mg/kg; IV). Hair was clipped from the dorso-lateral surface of both metacarpal areas and both thoracic walls in each horse. Local anesthesia was performed using 2% lidocaine hydrochloride. Four 2 cm x 2 cm (4cm^2) areas on the dorso-lateral surface of each metacarpal area beginning just above the metacarpophalangeal joint, and on each lateral thoracic wall, 1.5 cm apart in a staggered vertical column were traced out and excised using a scalpel. These wounds were left to heal by second intention, and were bandaged postoperatively for 24 hours to control hemorrhage. After 24 hours, bandages were removed and viral therapy was administered to four wounds of one randomly assigned metacarpal area and one thoracic area.

The viral therapy was extrapolated from previous mice experiments (Wise *et al*., 2012; Wise *et al*., 2014) so that vIL-10 and VEGF-E (1 µg and 10 µg of each respectively, in 200 mL PBS) were administered by subcutaneous injection adjacent to each border of each treated wound at 24, 48 and 72 hours. Full-thickness wound margin

samples were collected with an 8 mm diameter biopsy punch from one wound per site (body; limb; control; treated) at the time of wounding and after 48 hours, 7 days, 14 days, and at final wound closure. These biopsies were halved at right angles to the junction between the wound and the intact skin border. One half of each samples was incubated in RNAlater stabilisation solution (Invitrogen) for 24 h prior to being snap frozen in liquid nitrogen and stored at -80°C for later RNA isolation. The other half of each biopsy was fixed in neutral-buffered 10% formalin for 7 days, then stored in 70% ethanol until being processed in paraffin. All frozen and paraffin-embedded skin samples were then shipped to the University of Otago for analysis.

2.4.2 Quantitative PCR analysis of gene expression in equine skin

Individual skin samples were placed into a mortar and pestle with liquid nitrogen and ground into a fine powder, transferred into a 2 mL microfuge tube with 300 µL lysis buffer and homogenised with a 1 mL syringe and a 20-gauge needle. 1 mL Trizol (ThermoFisher) was added and mixed, then left to sit for 10 min. Chloroform (400 µL) was then added and mixed vigourously for 20 sec. The sample was left for 3 min then centrifuged at 13000 rpm at 4 °C for 20 min. Supernatant was removed and incubated at 56 °C for 10 min with 2 ng proteinase K. RNA was extracted following the protocol outlined by the Geneaid TriRNA Pure Kit, including an on column 15 min incubation with RNAse-free DNase I at room temperature. Any remaining DNA contamination was removed using Quanta Biosciences' PerfeCta DNase I (RNase-free) following the manufacturer's instructions. Synthesis of cDNA was conducted as described in section 2.2.5.

Quantitative PCRs were conducted using cDNA equivalent of 5ng RNA, the SYBR GreenER qPCR SuperMix (Invitrogen) and the Applied Biosystems 7500 Fast PCR machine, using primers in Appendix 1, Supplementary Table 1. Primer

efficiencies were determined and expression levels of genes were determined relative to GAPDH and to the levels in equine skin prior to wounding.

2.4.3 Histological analysis of equine skin wounds

Paraffin-embedded equine skin biopsies were trimmed of excess paraffin then cut into 4 μm sections using a microtome (Leica RM2025). The sections were mounted on DAKO slides for immunohistochemistry or Histobond slides (Marienfeld) for histological stains, and dried at 37 °C overnight.

Paraffin-embedded sections were deparaffinised by washes in Xylene, and rehydrated by sequential washes in 100%, 95% and 70% ethanol then into water. The sections were stained for 2 min with Celestin blue and Haemotoxylin, washed in Scott's water and rinsed in 95% ethanol. Next the sections were stained for 5 min with 0.5% Martius Yellow in 95% ethanol, washed in water, stained for 10 min in 1% Crystal Scarlet in 2.5% acetic acid, washed again in water then treated with 1% phosphotungstic acid for 2 min. After a water wash, sections were counterstained for 2 min in Methyl Blue solution diluted 1 in 10 in 1% acetic acid, then rinsed in 1% acetic acid. The sections were dehydrated in 100% ethanol followed by a Xylene wash. Coverslips were mounted over the stained sections, sealed with clear nail polish and allowed to dry. The Histology Services Unit in the Pathology Department of the University of Otago performed the staining process. Photographs of the stained sections were taken at 4 X magnification using the upright microscope (Olympus BX-51) and cellSens software. Panoramics were generated using Adobe Photoshop.

Changes in epidermal repair were analysed in each section using Image J. The length of the neo-epidermis was measured on the boundary with the dermis from the edge of the normal skin into the wound tissue. The thickness of the neo-epidermis was calculated as the mean of five measurements equally spanning the length of new

epidermis. The length of each rete ridge (epidermal projection entering the dermis) was measured and the sum of all rete ridge lengths for each section was calculated.

2.4.4 Immunofluorescent analysis of equine skin wounds

Paraffin sections were dehydrated by incubation overnight at 37 °C. They were deparaffinised in Xylene for 15 min, and rehydrated by sequential washes in 100% ethanol, 100% propan-1-ol, 90% propan-1-ol, and 70% propan-1-ol. Slides were then washed in 0.85% NaCl solution and re-equilibriated in PBS for 30 min. At this point, antigen retrieval methods varied for each antibody. Sections that were to be used with antibodies against α-smooth muscle actin (αSMA) or von-Willebrand factor (vWF) were placed in TBS pH 7.4 at 37 °C for 20 min. Sections that were to be used with antibodies against major histocompatibility complex (MHC-II) were incubated in 10 mM sodium citrate pH 6 at 95 °C for 20 min using a decloaking chamber (Biocare). All sections were placed in room temperature TBS for 20 min prior to staining. Sections were incubated with the primary antibodies at the appropriate dilution, at the specified temperature in a dark, humid chamber, for the specified time, as listed in table 1. Where necessary this was followed by incubation with a secondary antibody following the conditions listed in table 1. For the final 30 min of the incubation, 80 µL of DAPI (75 nM) was added. The sections were then rinsed in TBS and mounted in 10 µL SlowFade Gold before placement of the coverslips on microscope slides and storage at 4°C overnight. Stained sections were photographed at 4 X or 10 X magnification using the upright Olympus BX-51 fluorescence microscope using the cellSens Software. Panoramics were generated of each section using Adobe Photoshop.

For sections incubated with antibodies against vWF and αSMA, the area of positive staining within the newly formed granulation tissue (wound dermis) was calculated as a percentage of the total granulation tissue area on ImageJ. The

percentage area that was stained positive for MHC-II was calculated as a proportion of the total section area (normal and wound tissue).

Table 1. Antibody dilutions, incubation times and clone identification.

Antibody (Clone)	Dilution (80 µL volume)	Incubation Time	Company (Cat. No.)
Primary			
Mouse α-αSMA-Cy3 (1A4)	1:400	2 hours RT	Sigma-Aldrich C6198
Rabbit α-human vWF (polyclonal)	1:200	2 hours RT	DakoCytomation A 0082
Mouse α–equine MHC-II (CVS20)	1:50	Overnight 4°C	Abcam ab23206
Rabbit α -Vimentin-Alexa Fluor488 (D21H3)	1:50	2 hours RT	Cell Signalling 9854
Secondary			
Goat α-rabbit 488	1:500	1 hour RT	Invitrogen A-11034
Goat α-mouse 488	1:500	1 hour RT	Invitrogen A-110001

2.5 Statistical analysis

Statistical analysis of the data obtained from treated and untreated equine skin wounds at individual time points were performed using a paired *T*-test when matching samples from each horse were available, and using an unpaired *T*-test when matching samples were unable to be generated. Normal distribution could not be determined from the 4 samples, as this number is too small.

3 Results

3.1 *In vitro* analysis of viral protein activity in equine cells

The initial objective of this project was to determine the effects of the viral proteins on equine cells. The first step was therefore to produce the recombinant viral proteins, VEGF-E and vIL-10, for use in bioassays. An equine fibroblast cell line was then generated from skin biopsies taken from the thoracic (body) and metacarpal (limb) regions of thoroughbred horses for use in bioassays. As the viral proteins have both been shown to regulate inflammation and fibrosis (Wise *et al*., 2012; Wise *et al*., 2014), quantitative PCR was used to examine the effects of VEGF-E and vIL-10 on equine fibroblast gene expression. As the mammalian equivalents of the viral proteins have been shown to regulate fibroblast proliferation and migration (Zhao *et al*., 2013; Zhao *et al*., 2014), a scratch assay was used to examine the effects of VEGF-E and vIL-10 on equine fibroblast activity.

3.1.1 Production of the viral proteins

FLAG-tagged VEGF-E and vIL-10 were purified from supernatant of HEK293-EBNA cell lines via affinity chromatography and ultracentrifugation. Purified protein was resolved on an SDS-PAGE, stained with Coomassie blue. Band densities were compared to a standard curve generated using a protein of known concentration (CA). Figure 1 shows two bands of 25 and 28 kDa, which are consistent with the molecular weight (MW) reported for VEGF-E (Wise *et al*., 1999). A band was also observed at 20 kDa that is consistent with the MW of vIL-10 reported previously (Imlach *et al*., 2002). Concentrations of VEGF-E and vIL-10 were found to be 150 and 120 ng/µL, respectively.

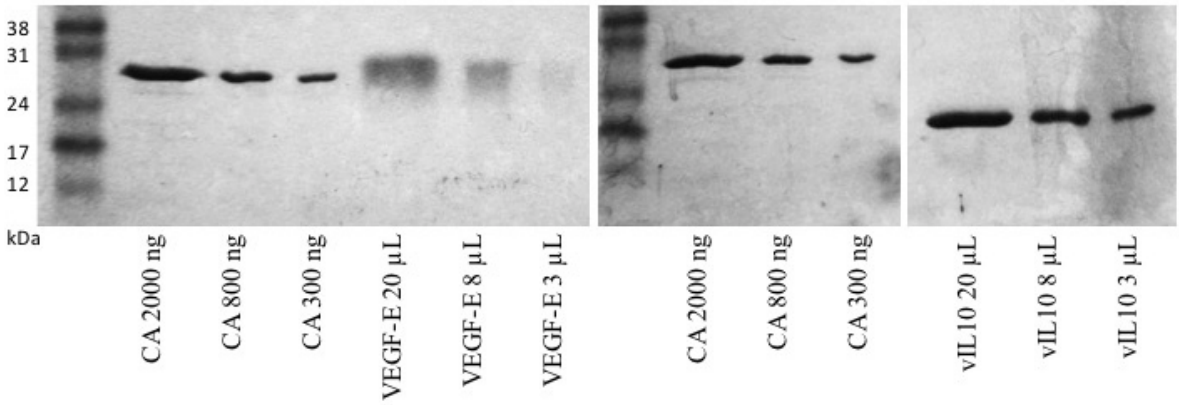

Figure 1. SDS-page quantitation gels of purified VEGF-E and vIL-10 protein. Varying amounts of carbonic anhydrase (CA, 100 ng/µL), VEGF-E and vIL-10 were resolved by SDS-PAGE and stained with Coomassie blue for quantification using densitometry. Size of the rainbow marker are indicated.

3.1.2 Generation of an equine cell line

Three extraction methods and two culture medias were trialed for the extraction of skin cells, as described in materials and methods (Table 2). Brick-shaped cells that resembled keratinocytes were obtained from the equine skin explants but these cells were out competed by fibroblasts. Similar cells were also obtained following collagenase/dispase digestion of the body skin but in this case the cells were unable to be passaged more than five times. In contrast, spindle-shaped cells that resembled fibroblasts were able to be cultured from body and limb skin from each extraction method and using either grown media.

Table 2. Table showing outcome of cell growth from each extraction method. Crosses indicate cells that failed to grow beyond passage 1, ticks indicates methods that isolated pure colonies that could be passaged.

		Trypsin incubation	Collagenase/dispase incubation	Gelatin explants
eKGM	Keratinocytes	✓	✓ - up to P5	✓- up to P5
	Fibroblasts	✓	✓	✓
eFGM	Keratinocytes	✗	✗	✓- up to P5
	Fibroblasts	✓	✓	✓

eKGM = equine keratinocyte growth media. eFGM= equine fibroblast growth media.

Two fibroblast-like cell lines, generated from limb and body skin, were examined in more detail. To confirm whether the cell lines were indeed fibroblasts, these cells were stained with fluorescent antibodies against Vim, which is present in the intermediate filaments of fibroblasts (Theoret *et al*., 2013), and αSMA, which is used to differentiate fibroblasts with myofibroblasts (Theoret *et al*., 2013) (Fig. 2A). Both the limb and body cell lines stained 100% positive for Vim, while approximately 50% of cells were also positive for αSMA (Fig. 2A). These findings illustrate that the equine cell lines contained a mixture of both fibroblasts and myofibroblasts.

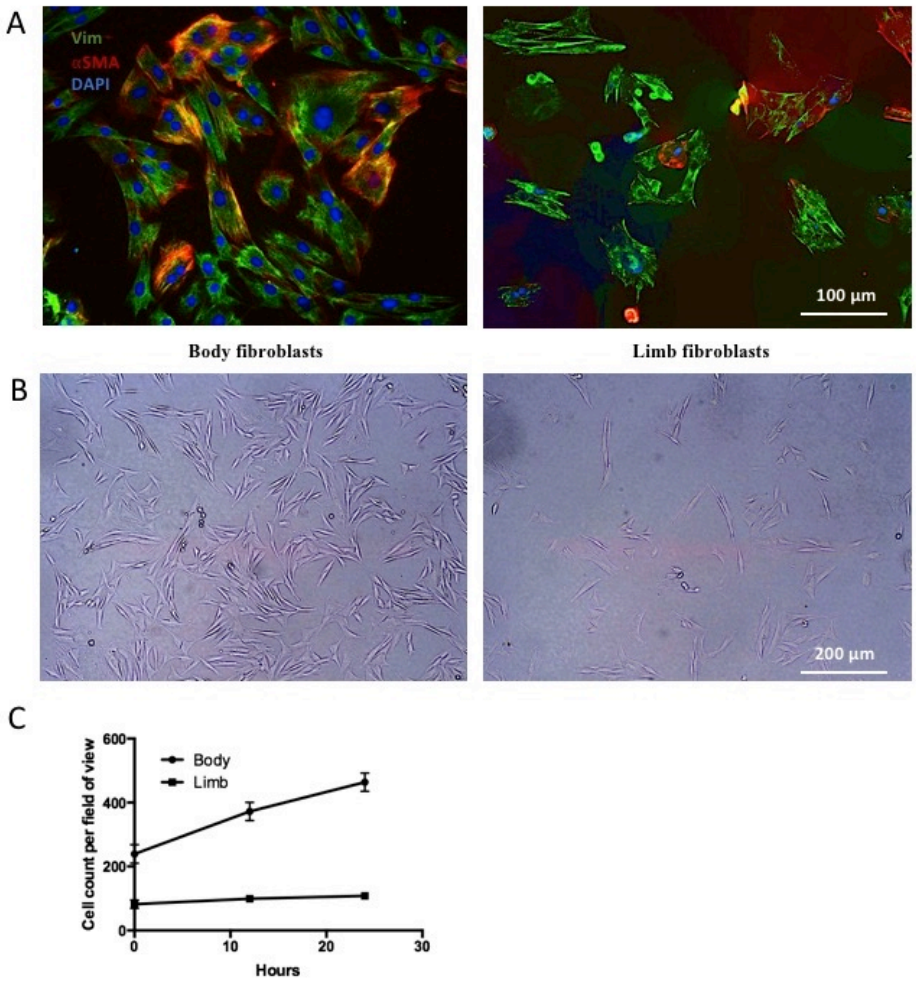

Figure 2. Immunofluorescent and growth analysis of equine cell lines. (A) Images of limb and body cells stained with fluorescent antibodies against vimentin (Vim; fibroblasts), α-smooth muscle actin (α-SMA; myofibroblasts) and a nuclear stain (DAPI). Scale is indicated. (B) White light images of limb and body cells taken at 10X magnification. (C) Growth curve of cells over a 24 h period. Cells per field of view were counted (n = 3). Values represent the mean ± SEM. Scale is indicated.

A growth curve was conducted on the fibroblast cell lines originating from limb and body skin (Fig. 2B-C). The body fibroblasts doubled in number within the 24 h period, while the limb fibroblasts showed very limited proliferation during that time frame (Figure 2B-C). From this point, all assays were performed using the faster growing equine body fibroblasts.

To ensure the equine body fibroblasts would be responsive to the viral proteins, PCR analysis for the expression of the appropriate VEGF and IL-10 receptors was performed. A PCR was conducted on RNA extracted from the cells using primers for VEGFR1, VEGFR2 and IL-10Rα and the products were visualised on an agarose gel (Fig. 3). The cell line was shown to express all three of the receptors, showing bands of ~100 bp which is consistent with the product size expected from these primers (Fig. 3). A smaller, fainter band was also observed in the no template control well, which was consistent with a dimer forming with the VEGFR-1 primers (Fig. 3).

These findings demonstrate that a proliferative equine cell line was successfully generated that expressed fibroblast markers and the receptors necessary for viral protein activity.

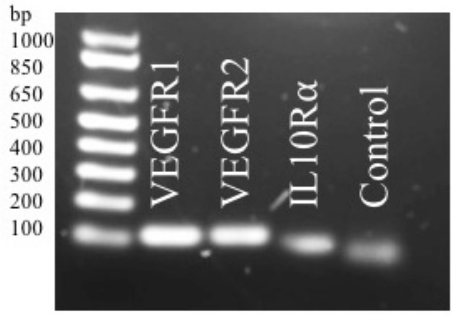

Figure 3. PCR analysis of VEGF and IL-10 receptor expression in equine body cells. Bands for VEGFR1, VEGFR2, IL-10Rα and control (VEGFR1 primers + no template) are indicated. 1 kbp marker is shown.

3.1.3 Effects of viral proteins on equine fibroblast gene expression

Primers were designed for quantitative PCR analysis of genes regulating inflammation and fibrosis (equine (e)MIP-2α, eMCP-1, eTNFα, eMMP-1, eCol1α2, eαSMA, eVEGF-A, eIL-10, eTGFβ1 and eTGFβ3). Primer pairs were tested using cDNA generated from total RNA extracted from the equine body fibroblasts. Primer pairs with efficiencies closest to 100% (100 ± 30%) were chosen for the analyses (Appendix 1, Supplementary Table 1). The equine fibroblasts were then treated either with VEGF-E or vIL-10 alone, or co-treated with polyinosinic:polycytidylic acid (polyI:C) to promote an inflammatory response (Hamidi *et al*., 2014). Total RNA was then extracted, cDNA synthesised and gene expression analysed using quantitative PCR.

Changes in the expression of genes involved in inflammation (eMIP-2α, eMCP-1 and eTNFα) following treatment with the viral proteins with or without polyI:C are shown in Figure 4. The expression of the inflammatory chemokine eMIP-2α and eMCP-1 increased following treatment with PolyI:C (Fig. 4A-B) while very little change was observed in the expression of the inflammatory cytokine eTNFα (Fig. 4C). Treatment with vIL-10 decreased the expression of eTNFα, in the presence and absence of polyI:C (Fig. 4C), but in contrast increased the expression of eMCP-1 in the presence of polyI:C (Fig. 4B). No change in expression was observed following VEGF-E treatment for any of the genes (Fig. 4).

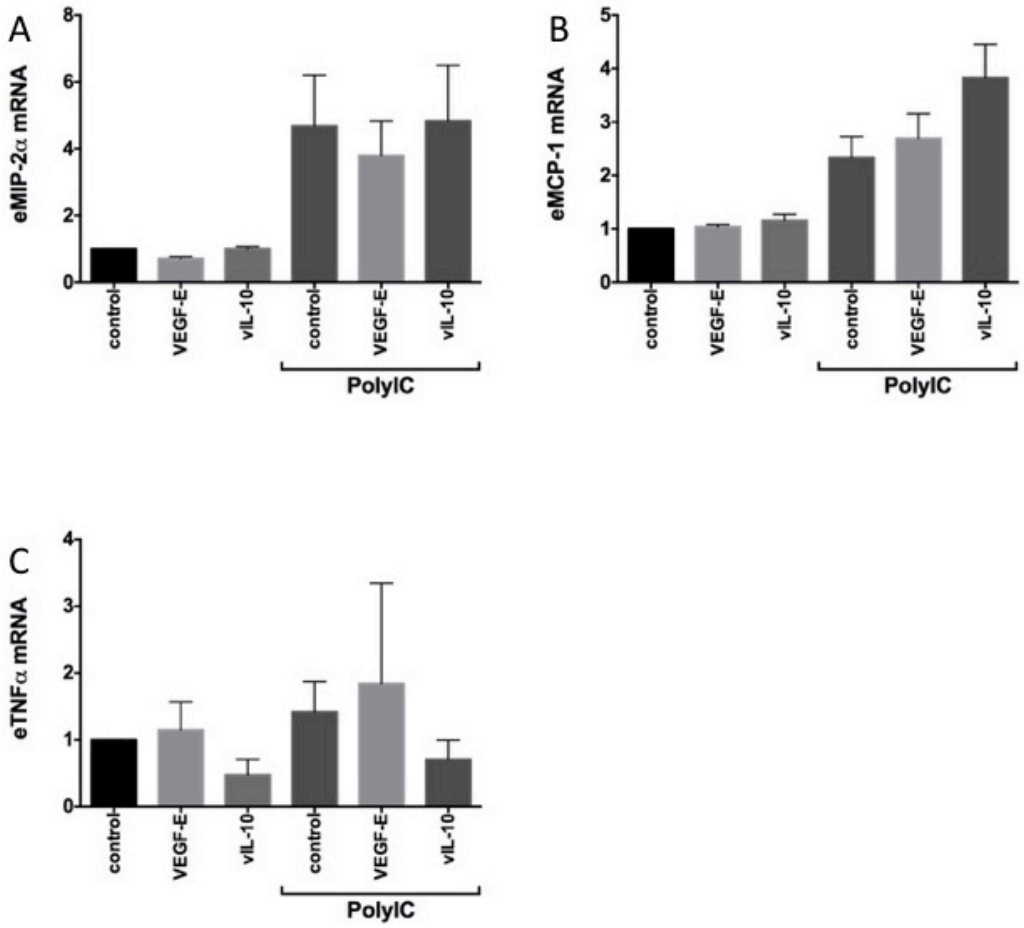

Figure 4. Inflammatory gene expression in equine body fibroblasts in response to VEGF-E or vIL-10. Cells were stimulated with VEGF-E (200 ng/mL), vIL-10 (20 ng/mL) or no protein control in media containing 0.1% BSA. Where indicated, polyI:C (50 μg/mL) was added concurrently to stimulate an inflammatory response. After 2 h incubation, cells were harvested, total RNA extracted and cDNA synthesised. Quantiative PCR analysis was then used to detect expression of (A) equine (e)MIP-2α, (B) eMCP-1 and (C) eTNFα. Expression of mRNA is relative to that of eGAPDH and to the control unstimulated cells. Values represent mean ± SEM (n = 2, mean of duplicates from two replicate experiments).

Changes in the expression of genes involved in fibrosis (eMMP-1, eαSMA and eCol1α2) following treatment with the viral proteins are shown in Figure 5. Treatment with vIL-10 increased the expression of eMMP-1 (Collagenase-1, Fig. 5A), but had no effect on fibroblast expression of eαSMA or eCol1α2 (Fig. 5B-C). No change in expression was observed following VEGF-E treatment for any of the genes (Fig. 5).

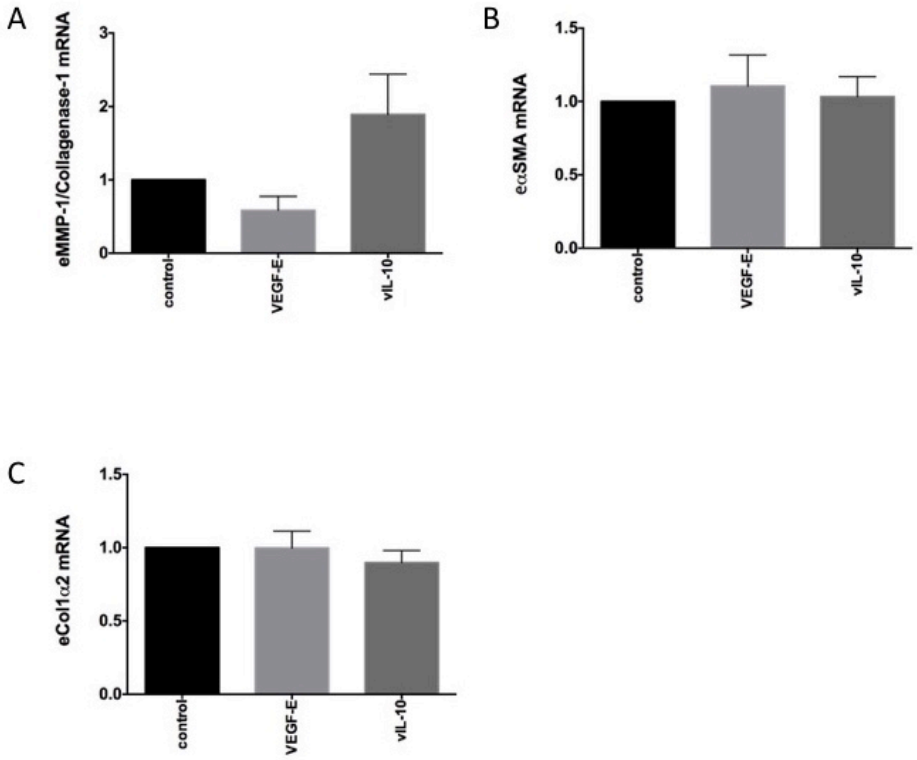

Figure 5. Fibrosis-related gene expression in equine body fibroblasts in response to VEGF-E or vIL-10. Cells were stimulated with VEGF-E (200 ng/mL), vIL-10 (20 ng/mL) or no protein control in media containing 0.1% BSA. After 2 h incubation, cells were harvested, total RNA extracted and cDNA synthesised. Quantiative PCR analysis was then used to detect expression of (A) equine (e) MMP-1, (B) eαSMA and (C) eCol1α2. Expression of mRNA is relative to that of eGAPDH and to the control unstimulated cells. Values represent mean ± SEM (n = 2, mean of duplicates from two replicate experiments).

Changes in the expression of key regulatory genes (eVEGF-A, eIL-10, eTGFβ1 and eTGFβ3) which control fibroblast proliferation, migration and differentiation following treatment with the viral proteins with or without polyI:C are shown in Figure 6. PolyI:C treatment increased expression of eVEGF-A, eIL-10, eTGFβ1 and eTGFβ3 compared to the unstimulated control cells (Fig. 6). VEGF-E treatment had no effect on the expression of eVEGF-A (Fig. 6A), and increased the expression of eIL-10, although a decrease in expression was observed in the presence of polyI:C (Fig. 6B). VEGF-E treatment also slightly decreased expression of eTGFβ1 and eTGFβ3, but this decrease was not observed after stimulation with polyI:C (Fig. 6C-D). Viral IL-10 treatment increased expression of eVEGF-A and eIL-10 (Fig. 6A-B). Treatment with vIL-10 also

decreased expression of eIL-10, eTGFβ1 and eTGFβ3 after stimulation with polyI:C (Fig. 6B-D).

These findings indicate that the viral VEGF-E, to some extent, altered the expression of regulatory genes in equine fibroblasts but did not impact the expression of genes involved in inflammation or fibrosis. The viral IL-10 dampened the expression of the eIL-10, the eTGFβ isoforms and eTNFα by polyI:C, and increased expression of the degradative enzyme, eMMP-1, in unstimulated equine fibroblasts.

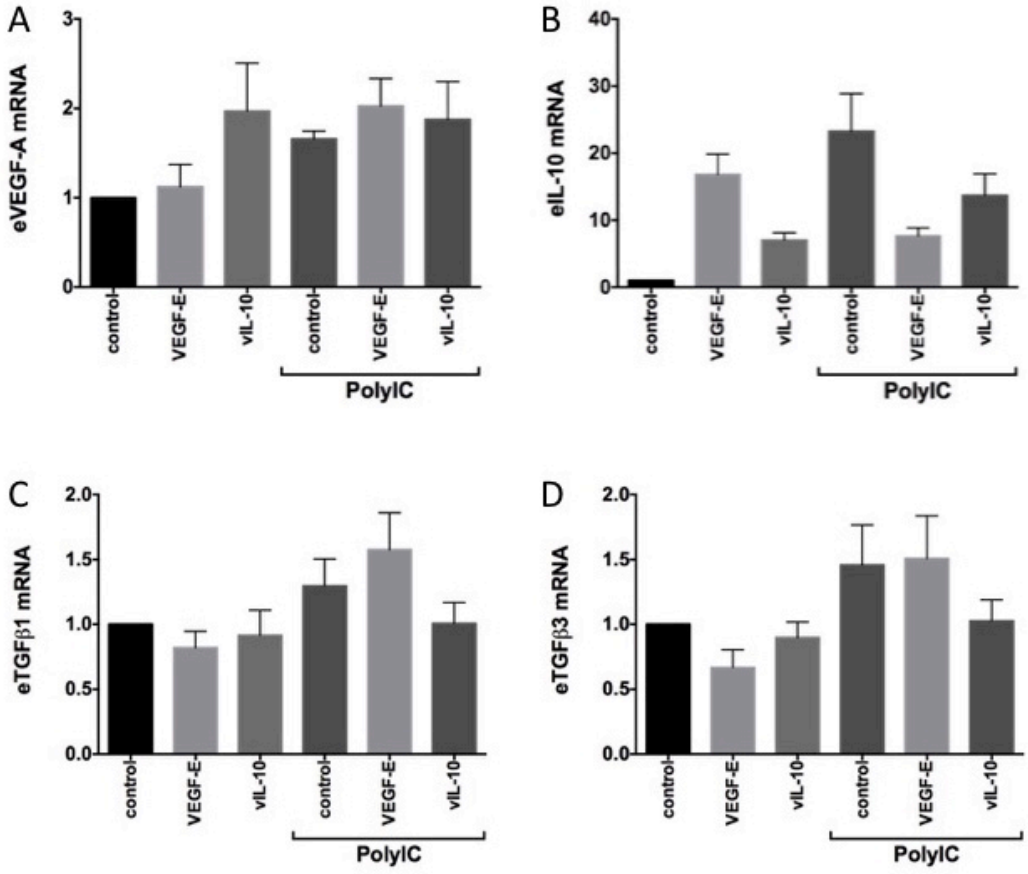

Figure 6. Regulatory genes in equine body fibroblasts in response to VEGF-E or vIL-10. Cells were stimulated with VEGF-E (200 ng/mL), vIL-10 (20 ng/mL) or no protein control in media containing 0.1% BSA media. Where indicated, polyI:C (50 μg/mL) was added concurrently to stimulate an inflammatory response. After 2 h incubation, cells were harvested, total RNA extracted and cDNA synthesised. Quantiative PCR analysis was then used to detect expression of (A) eVEGF-A, (B) eIL-10, (C) eTGFβ1 and (D) eTGFβ3. Expression of mRNA is relative to that of eGAPDH and to the control unstimulated cells. Values represent mean ± SEM (n = 2, mean of duplicates from two replicate experiments).

3.1.4 Effects of viral proteins on equine fibroblast migration

Mammalian VEGFs and IL-10 have both been shown to influence the proliferation and migration of human fibroblasts, in a positive and negative manner, respectively (Moroguchi *et al*., 2004; Zhao *et al*., 2013; Zhao *et al*., 2014). In order to determine if the viral factors influenced the equine fibroblasts in the same manner, an *in vitro* scratch assay was performed (Rose, 2012).

Fibroblasts were grown to confluence then a scratch was administered down the centre of each well and photos were taken of the cells migrating to close the wound (Fig. 7A). The rate of closure over time was calculated and showed that, in the presence of 1% FCS, the cells had filled the scratch within 48 h (Fig. 7B-C). In contrast, cells in the presence of 0.1% BSA had filled only 20% of the scratch area within 48 h (Fig. 7B-C). The addition of VEGF-E or vIL-10 to the media containing 0.1% BSA did not, over the 48 h period, reduce scratch area from that of the control (Fig. 7B-C). The cells treated with vIL-10 did however survive the serum-free conditions better than the cells in media containing 0.1% BSA alone (n =5-6, three replicated experiments).

The results indicate that the vIL-10 and VEGF-E do not significantly impact equine fibroblast proliferation and migration.

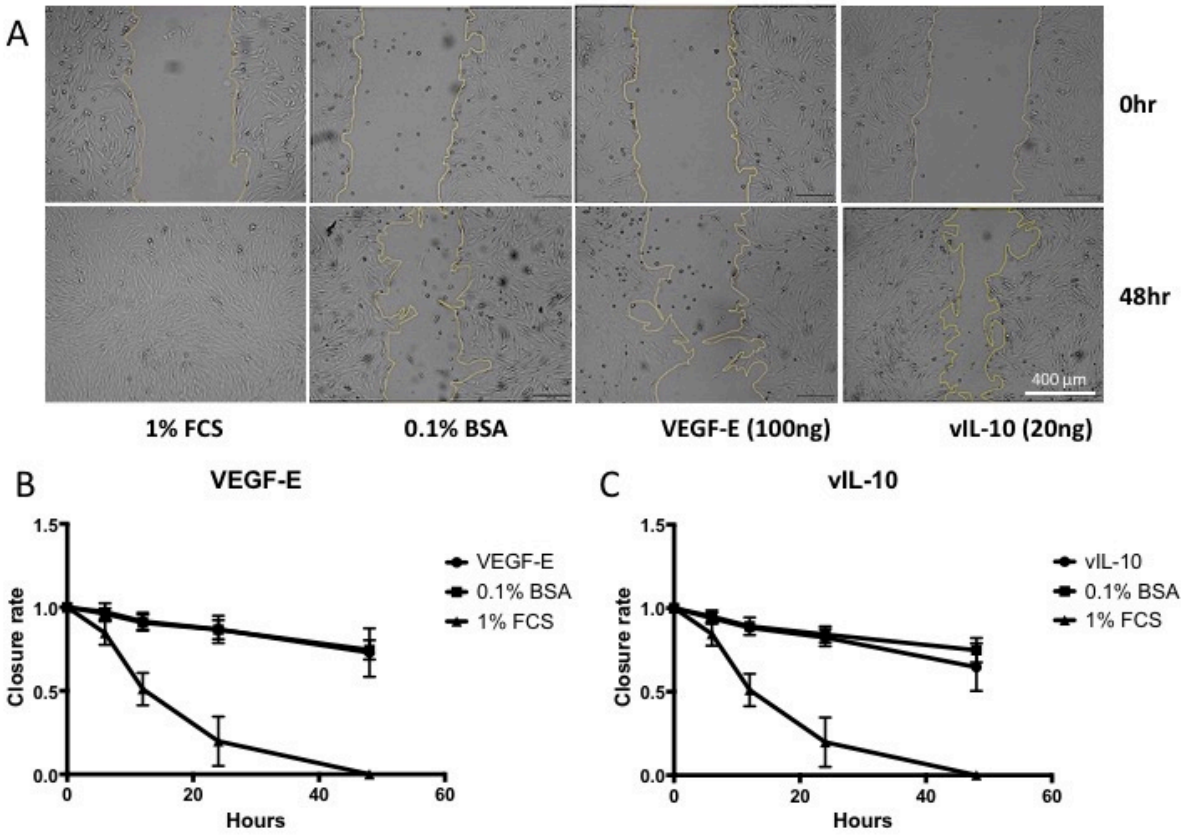

Figure 7. Cellular migration of equine body fibroblasts in response to VEGF-E or vIL-10. Confluent fibroblasts were scratched with a 600 µm wide pipette tip then incubated with DMEM containing either 1% FCS, 0.1% BSA, or 100 ng VEGF-E or 20 ng vIL-10 with 0.1% BSA. (A) White light images taken at 10X magnification. Closure rate following (B) VEGF-E or (C) vIL-10 treatment. The closure rate was calculated as a ratio between the area of the scratch at each time point compared with the original scratch area. Values represent mean ± SEM (n=13-18 wells from three replicate experiments).

3.2 *In vivo* analysis of viral protein activity in equine skin wounds

The second objective of this project was to determine the effects of the viral proteins on equine skin wounds. In a trial at Massey University, four thoroughbred horses each received four skin wounds on both metacarpal areas (limb) and on both thoracic walls (body). Body wounds heal efficiently while limb wounds become chronic in nature. At 24, 48 and 72 h post surgery, wounds were randomly administered VEGF-E and vIL-10 (10 and 1μg, respectively, in 200 μL PBS) to one limb and one body region, while the matching regions received the control treatment (200 μL PBS). Biopsies were taken from a single wound in each region at day 2, 7 and 14, and at the time of closure.

The viral proteins have both been shown to regulate inflammation, repair and remodelling (Wise *et al*., 2012; Wise *et al*., 2014), so quantitative PCR was used to examine the effects of VEGF-E and vIL-10 on equine skin wound gene expression. As the viral proteins have been shown to regulate wound re-epithelialisation (Wise *et al*., 2012; Wise *et al*., 2014), histological analyses were used to examine the effects of VEGF-E and vIL-10 on the regenerating epidermis in the equine wounds. Because the viral proteins have been shown to influence wound re-vascularisation (Wise *et al*., 2012; Wise *et al*., 2014), immunofluorescent analyses were used to determine the effects of VEGF-E and vIL-10 on blood vessel formation in the equine wounds. The viral proteins have also been shown to influence immune cell trafficking (Wise *et al*., 2012; Wise *et al*., 2014), therefore immunofluorescent analyses were used to evaluate the effects of VEGF-E and vIL-10 on antigen-presenting cells within the equine wounds.

3.2.1 Effects of the viral proteins on equine skin wound gene expression

Additional primers were designed for quantitative PCR analysis of genes regulating inflammation, repair and remodelling (eFPR2, eIL-10Rα, eCTGF, eSPP-1, eCol3α1, ePDGF-β, eIL-10, eVEGFR-1 and eVEGFR-2). Primer pairs were tested using cDNA generated from total RNA extracted from the equine body fibroblasts. Primer pairs with efficiencies closest to 100% (100 ± 30%) were chosen for these analyses (Appendix 1, Supplementary Table 1). Total RNA was then extracted from biopsies taken of the treated and control chronic limb wounds taken at each time point, cDNA was synthesised and gene expression analysed using quantitative PCR.

Changes in the expression of pro-inflammatory genes (eMCP-1, eMIP-2α, eTNFα and eFPR2) in chronic limb wounds following treatment with the viral proteins are shown in Figure 8. Expression of the chemokines, eMCP-1 and eMIP-2α, peaked at day 2 and was still above that of unwounded skin at the time of closure (Fig. 8A-B). Expression of the cytokine eTNFα showed a slight decrease over time and was below that of unwounded skin at the time of closure (Fig. 8C). Expression of the chemotactic neutrophil receptor eFPR2 peaked at day 2 and had returned to the level of unwounded skin by the time of closure (Fig. 8D). Treatment with the VEGF-E and vIL-10 led to an immediate decrease in the expression of eMCP-1, eMIP-2α and eTNFα compared with the control wounds at 2 days (Fig. 8A-C, P = 0.01-0.07). No clear differences in the expression of the inflammatory genes were observed between control and treated wounds at any other time point (Fig. 8).

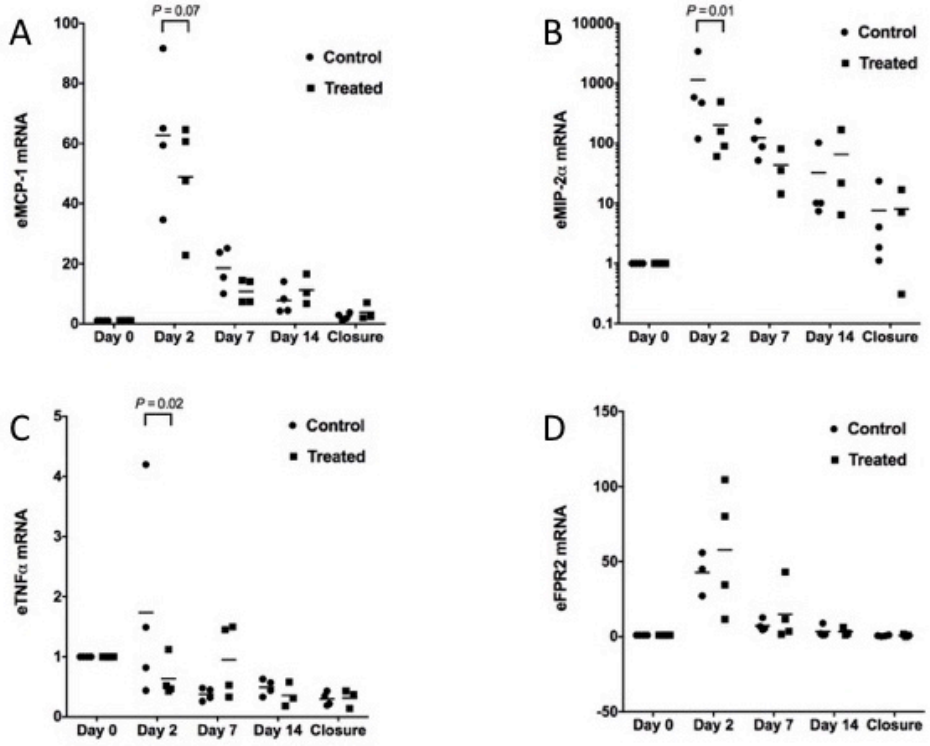

Figure 8. Inflammatory gene expression in chronic limb wounds in response to treatment with VEGF-E and vIL-10. Limb wounds were generated in horses then were treated at 24, 48 and 72 h with VEGF-E (10 µg) and vIL-10 (1 µg) in 200 µL PBS (treated), or with PBS alone (control). Biopsies of wounds were taken at various timepoints post surgery, total RNA extracted and cDNA synthesised. Quantitative PCR analysis was then used to detect expression of (A) eMCP-1, (B) eMIP-2α, (C) eTNFα and (D) eFPR2. Expression of mRNA is relative to that of eGAPDH and unwounded skin. Values represent mean ± SEM (n = 3-4 horses). An unpaired *t*-test was used to identify significant differences between control and treated horses at each time point and *P* values ≤0.1 are indicated.

Changes in wound expression of the anti-inflammatory genes eIL-10 and eIL-10Rα following treatment with the viral proteins are shown in Figure 9. Both genes showed a steady decrease in expression over time and were well below that of unwounded skin by wound closure (Fig. 9). Treatment with the VEGF-E and vIL-10 led to an immediate decrease in the expression of eIL-10 and a delayed decrease in eIL-10Rα at 2 and 7 days, respectively, compared with control wounds (Fig. 9, $P = 0.0005$-0.002). No clear differences in the expression of the anti-inflammatory genes were observed between control and treated wounds at any other time point (Fig. 9).

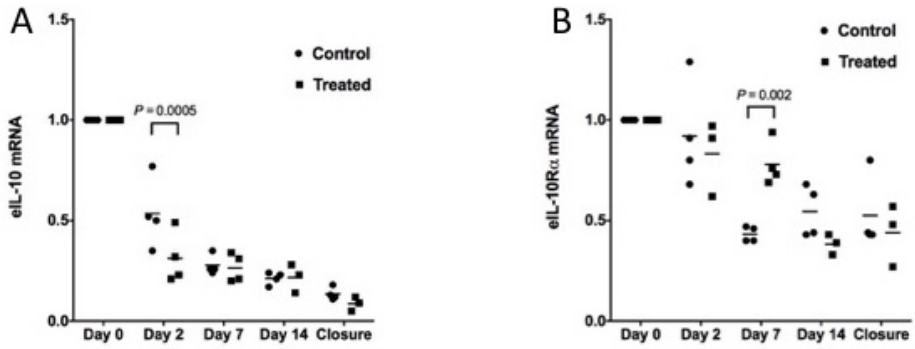

Figure 9. Anti-inflammatory gene expression in chronic limb wounds in response to treatment with VEGF-E and vIL-10. Limb wounds were generated in horses then were treated at 24, 48 and 72 h with VEGF-E (10 µg) and vIL-10 (1 µg) in 200 µL PBS (treated), or with PBS alone (control). Biopsies of wounds were taken at various timepoints post surgery, total RNA extracted and cDNA synthesised. Quantitative PCR analysis was then used to detect expression of (A) eIL-10 and (B) eIL-10Rα. Expression of mRNA is relative to that of eGAPDH and unwounded skin. Values represent mean ± SEM (n = 3-4 horses). A paired *t*-test was used to identify significant differences between control and treated horses at each time point and *P* values ≤0.1 are indicated.

Expression of wound repair genes (eVEGF-A, ePDGF-β, eVEGFR-1 and eVEGFR-2) following treatment of limb wounds with VEGF-E and vIL-10 is shown in Figure 10. Expression of eVEGF-A and ePDGF-β, mitogens for endothelial cells and keratinocytes, and pericytes, respectively, decreased over time and were well below that of unwounded skin at all time points (Fig. 10A-B). Expression of the VEGF receptors, eVEGFR-1 and eVEGFR-2 also decreased initially but eVEGFR-2, unlike eVEGFR-1, returned to that of unwounded skin by day 7 (Fig. 10C-D). Treatment with the VEGF-E and vIL-10 led to an imediate decrease in the expression of eVEGF-A, at day 2 compared with control wounds (Fig. 10A, $P = 0.02$). The viral protein treatment also caused a delayed reduction in the expression of eVEGFR-1 compared to control wounds at day 14 (Fig. 10C, $P = 0.03$). No clear differences in the expression of the

repair genes were observed between control and treated wounds at any other time point (Fig. 10).

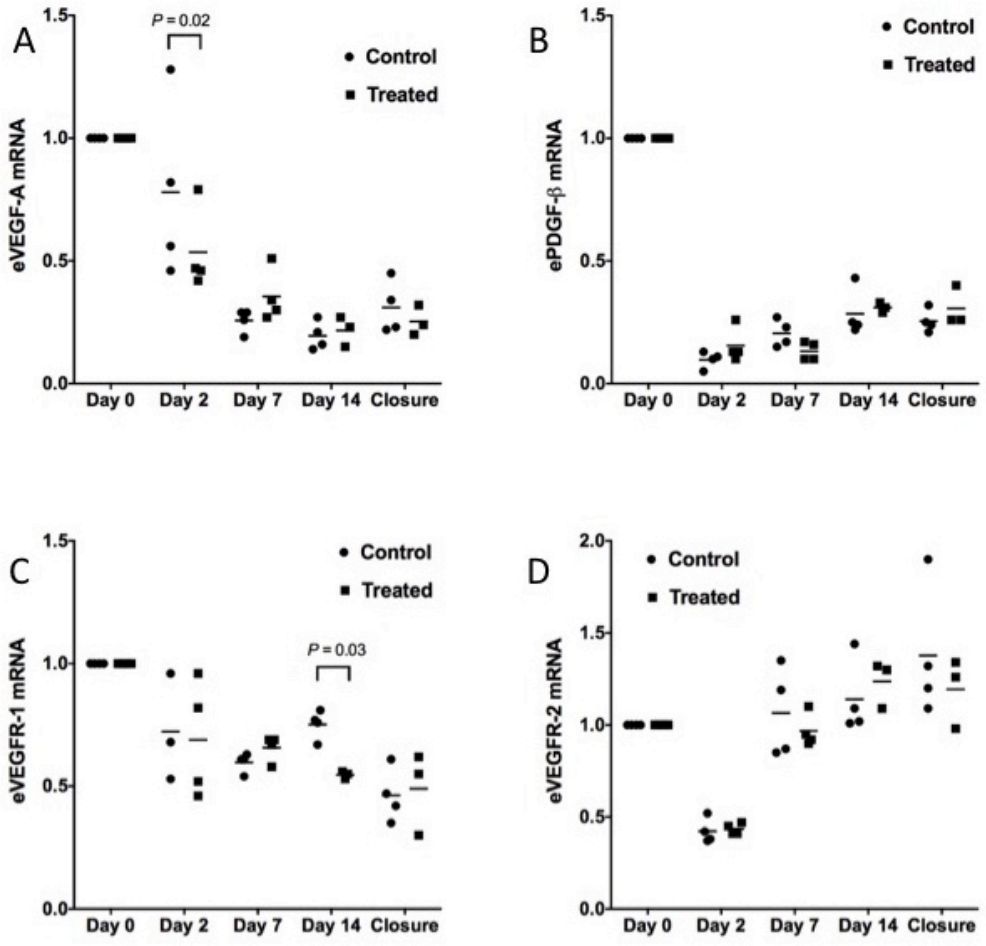

Figure 10. Repair gene expression in chronic limb wounds in response to treatment with VEGF-E and vIL-10. Limb wounds were generated in horses then were treated at 24, 48 and 72 h with VEGF-E (10 μg) and vIL-10 (1 μg) in 200 μL PBS (treated), or with PBS alone (control). Biopsies of wounds were taken at various timepoints post surgery, total RNA extracted and cDNA synthesised. Quantitative PCR analysis was then used to detect expression of (A) eVEGF-A, (B) ePDGFβ, (C) eVEGFR1 and (D) VEFGR2. Expression of mRNA is relative to that of eGAPDH and unwounded skin. Values represent mean ± SEM (n = 3-4 horses). An unpaired *t*-test was used to identify significant differences between control and treated horses at each time point and *P* values ≤0.1 are indicated.

Expression levels of regulatory genes involved in wound fibrosis (eCTGF, eSPP-1, eTGFβ1 and eTGFβ3) following treatment with VEGF-E and vIL-10 are

shown in Figure 11. Expression of the fibroblast mitogen eCTGF initially decreased at 2 days and began to increase back to the level of unwounded skin by the time of closure (Fig. 11A). Expression of the immune-stimulatory eSPP-1/Osteopontin also decreased at 2 days and remained below that of unwounded skin (Fig. 11B). Expression of the fibrosis regulators eTGFβ1 and eTGFβ3 initially decreased at 2 days, but increased to above that of unwounded skin by day 14 (Fig. 11C-D). Treatment with the VEGF-E and vIL-10 led to decreases in the expression of eSPP-1/osteopontin, eCTGF and the TGFβ isoforms at days 2, 7 and 14, respectively, compared with control wounds (Fig. 11, P = 0.001-0.07). No clear differences in the expression of the fibrosis genes were observed between control and treated wounds at any other time point.

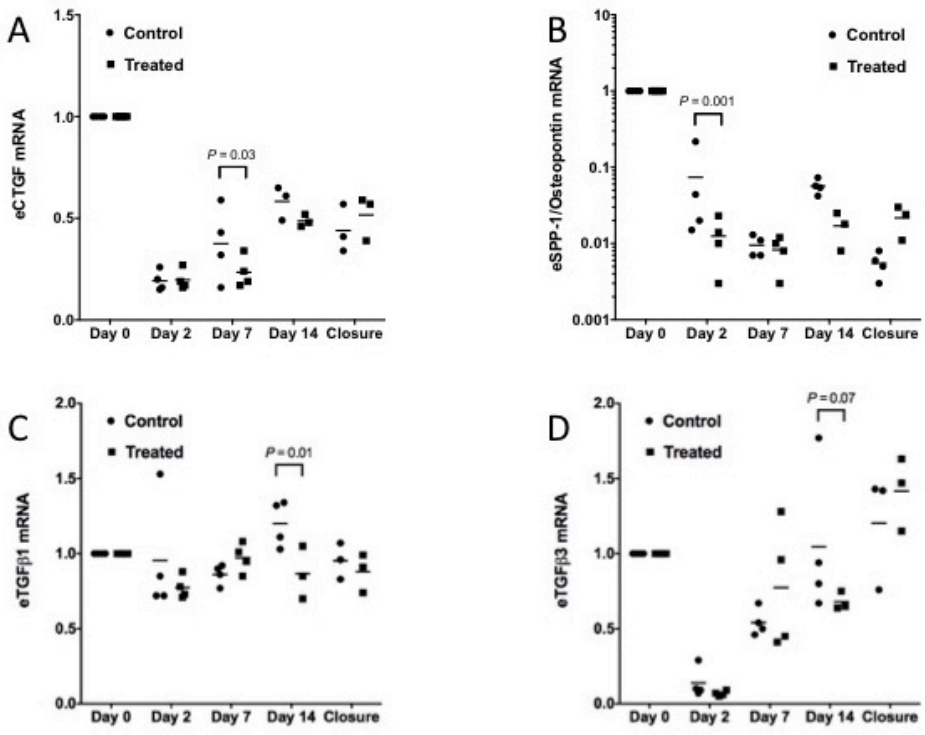

Figure 11. Fibrosis regulatory gene expression in chronic limb wounds in response to treatment with VEGF-E and vIL-10. Limb wounds were generated in horses then were treated at 24, 48 and 72 h with VEGF-E (10 µg) and vIL-10 (1 µg) in 200 µL PBS (treated), or with PBS alone (control). Biopsies of wounds were taken at various timepoints post surgery, total RNA extracted and cDNA synthesised. Quantitative PCR analysis was then used to detect expression of (A) eCTGF, (B) eSPP-1, (C) eTGFβ1 and (D) eTGFβ3. Expression of mRNA is relative to that of eGAPDH and unwounded skin. Values represent mean ± SEM (n = 3-4 horses). An unpaired *t*-test was used to identify significant differences between control and treated horses at each time point and *P* values ≤0.1 are indicated.

Extracellular matrix gene expression (eCol1α2, eCol3α1, eαSMA and eMMP-1) following treatment of limb wounds with VEGF-E and vIL-10 is shown in Figure 12. Expression of collagen types eCol1α2 and eCol3α1 increased over time and were at their highest level at the time of wound closure (Fig. 12A-B). Expression of the contractile protein eαSMA increased from day 2 to 14 and was closer to that of unwounded skin by the time of wound closure (Fig. 12C). Expression of the digestive enzyme eMMP-1/collagenase-1 was substantially increased between 2-14 days and was restored to that of unwounded skin by wound closure (Fig. 12D). Treatment with the VEGF-E and vIL-10 led to a decrease in the expression of eCol3α1, at day 7 compared with control wounds (Fig. 12B, $P = 0.02$). The viral protein treatment also altered the expression of eαSMA compared to control wounds with a decrease at day 7 (Fig. 11C, $P = 0.06$) and an increase at the time of wound closure (Fig. 12C, $P = 0.01$). No clear differences in the expression of the extracellular matrix genes were observed between control and treated wounds at any other time point (Fig. 12).

These results indicate that treatment with the VEGF-E and vIL-10 had a transient influence on the expression of key regulators of inflammation, repair and remodeling in equine skin wounds.

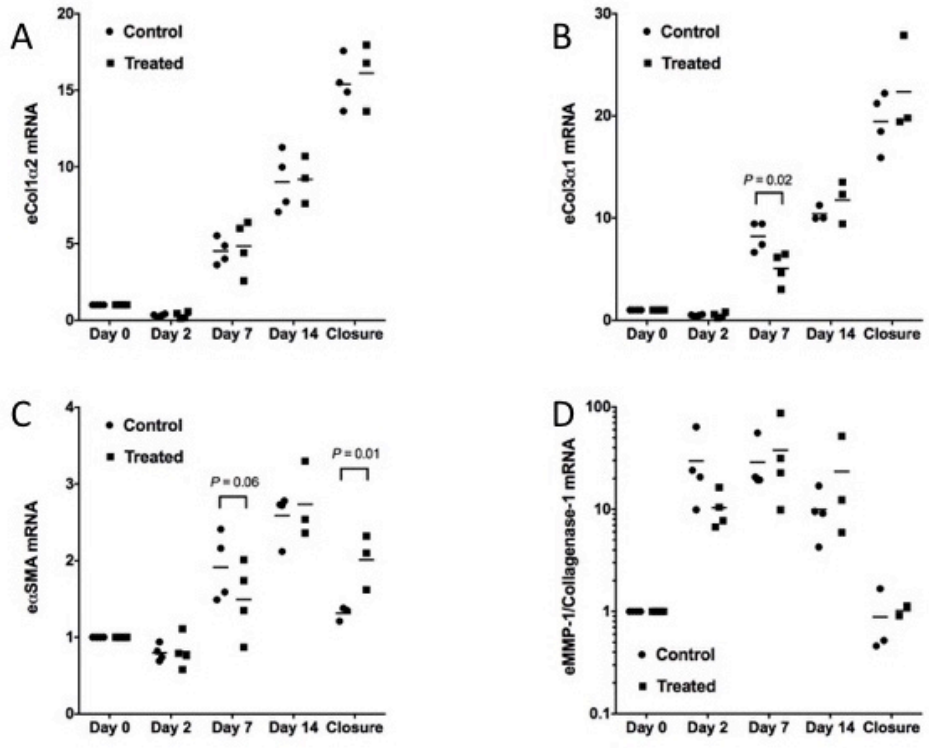

Figure 12. Extracellular matrix gene expression in chronic limb wounds in response to treatment with VEGF-E and vIL-10. Limb wounds were generated in horses then were treated at 24, 48 and 72 h with VEGF-E (10 μg) and vIL-10 (1 μg) in 200 μL PBS (treated), or with PBS alone (control). Biopsies of wounds were taken at various timepoints post surgery, total RNA extracted and cDNA synthesised. Quantitative PCR analysis was then used to detect expression of (A) eCol1α2, (B) eCol3α1, (C) eαSMA and (D) eMMP-1. Expression of mRNA is relative to that of eGAPDH and unwounded skin. Values represent mean ± SEM (n = 3-4 horses). An unpaired *t*-test was used to identify significant differences between control and treated horses at each time point and *P* values ≤0.1 are indicated.

3.2.2 Effects of the viral proteins on epidermal repair in equine skin wounds

In order to assess the effects of the viral treatment on the regenerating epidermis, zinc-fixed paraffin-embedded sections of biopsies taken from the limb and body wounds at each time point were stained with Martius Scarlet Blue (MSB). Figure 13 shows representative images of sections of control and treated chronic limb wounds taken at day 7, 14 and after final wound closure. Equivalent images of MSB-stained sections of body wounds are shown in Appendix 1, Supplementary Figure 1. After 7 days, a new epidermis was projecting from the wound edge in both body and chronic limb wounds and there was an increase in epidermal length observed in treated wounds when compared to controls (Fig. 13A, Sup. Fig. 1A). After 14 days, the new epidermis had thickened at the wound edge in the chronic limb wounds while this was not really observed in the body wounds (Fig. 13B, Sup. Fig. 1B). No difference in epidermal thickness was observed between treated and control wounds at this time (Fig. 13B, Sup. Fig. 1B). At the time of wound closure the epidermis had in general covered the entire wound bed but in chronic limb wounds there was an extensive network of epidermal projections (rete ridges) extending into the new dermis (Fig. 13C, Sup. Fig. 1C). No obvious difference in rete ridge formation was observed between treated and control wounds at this time (Fig. 13C, Sup. Fig. 1C).

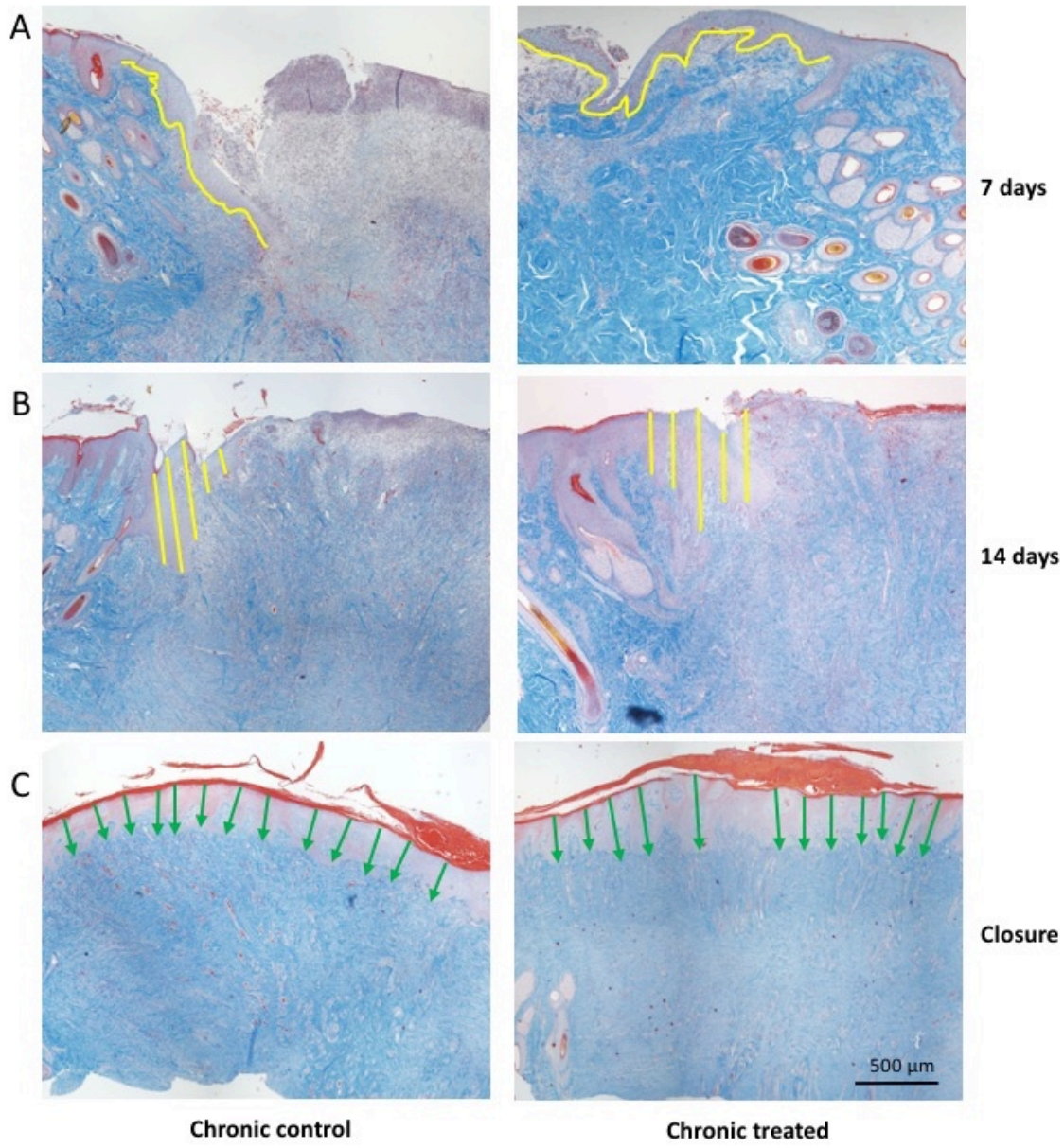

Figure 13. Epidermal repair in chronic limb wounds in response to treatment with VEGF-E and vIL-10. Images of MSB-stained sections from treated and control chronic limb wounds harvested at (A) 7 days, (B) 14 days and (C) at final wound closure. Fibrin is stained red and collagen stained blue. ImageJ software was used to measure the length (contoured yellow line illustrated in (A)), thickness (five yellow lines; thickness calculated as mean length of five lines illustrated in (B)) and rete ridge formation (green arrows; calculated as cumulative length illustrated in (C)) in the newly regenerating epidermis. Scale is indicated.

Image J was then used to analyse these physical changes observed in the regenerating epidermis of body and chronic limb wounds between those treated with VEGF-E and vIL-10 or the control. The length and thickness of the regenerating

epidermis was measured for each section as well as the cumulative length of all the rete ridges (Fig. 14). The epidermal length was similar in chronic and body wounds at day 7 and 14 but by wound closure the epidermal projections had substantially increased the overall length of the epidermis in the chronic wounds (Fig. 14A-B). Treatment with VEGF-E and vIL-10 had increased the length of the new epidermis after 7 days in both chronic limb and acute body wounds (Figure 14A-B, $P = 0.07$-0.09), but no differences were observed between the treated and control wounds after that point.

The epidermal thickness increased dramatically in chronic wounds at day 14 until wound closure but remained constant in the body wounds (Fig. 14C-D). Treatment with VEGF-E and vIL-10 increased the thickness of the new epidermis in body wounds after 7 days (Figure 14D, $P = 0.04$), but no differences were observed between the treated and control limb wounds (Fig. 14C).

Rete ridge formation also increased dramatically in chronic wounds from day 7 until wound closure but remained constant in the body wounds (Fig. 14E-F). Treatment with VEGF-E and vIL-10 however had no measurable effect on the cumulative length of the rete ridges compared to control wounds (Figure 14E-F).

These results indicate that treatment with the VEGF-E and vIL-10 induced a transient increase in epidermal repair in equine skin wounds.

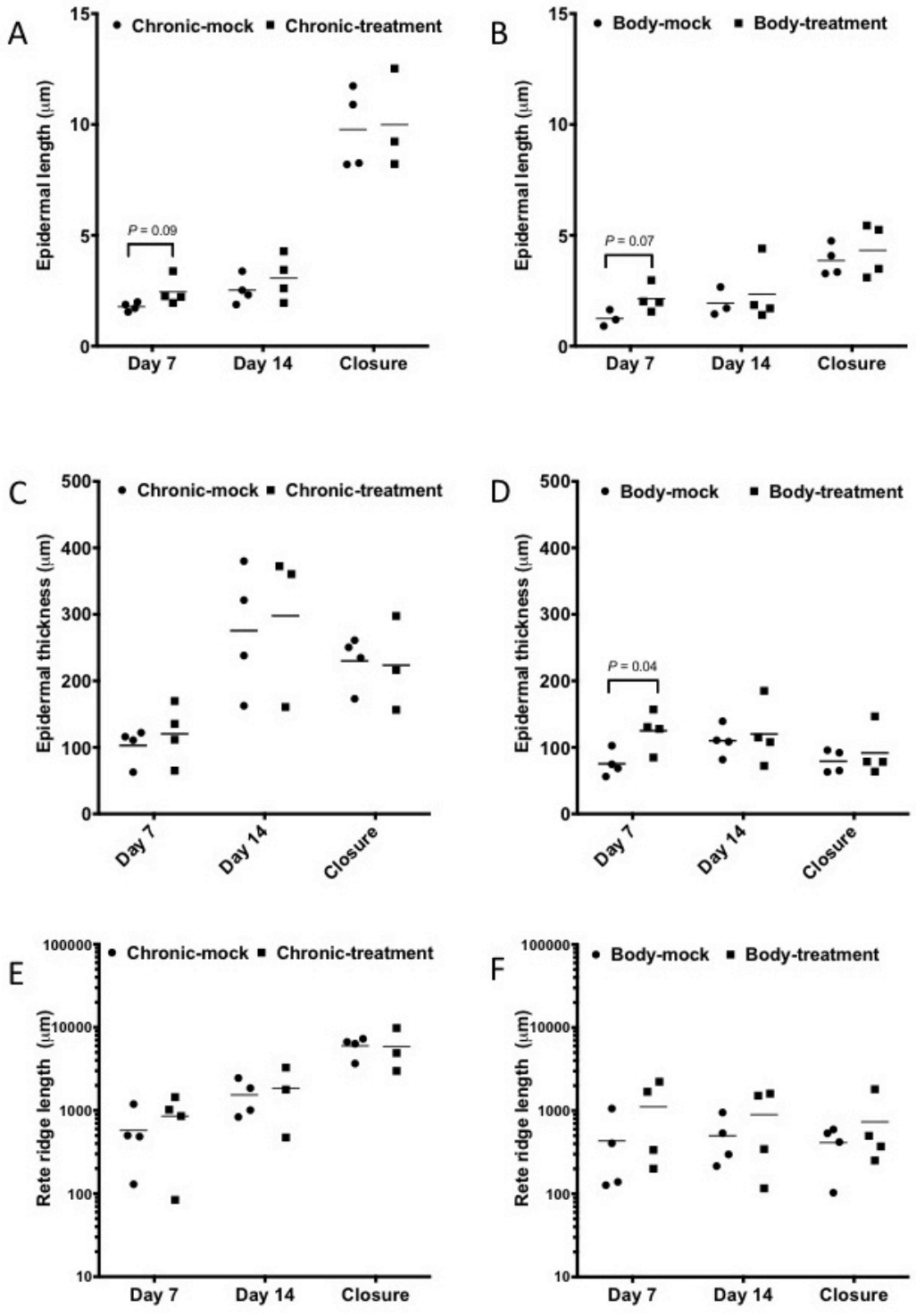

Figure 14. Quantification of epidermal repair in equine wounds in response to treatment with VEGF-E and vIL-10. ImageJ software was used to measure (A-B) epidermal length, (C-D) epidermal thickness and (E-F) rete ridge formation in MSB-stained sections from chronic (A, C, E) and body (B, D, F) equine wounds. Thickness is calculated as mean of five measurements and rete ridge formation is calculated as the cumulative length of all rete ridges. Values represent mean ± SEM (n = 3-4). An unpaired *t*-test was used to identify significant differences between control and treated horses at each time point and *P* values ≤0.1 are indicated.

3.2.3 Effects of the viral proteins on re-vascularisation of equine skin wounds

In order to assess the effects of the viral treatment on the production of new blood vessels, zinc-fixed paraffin-embedded sections of biopsies taken from the limb and body wounds at each timepoint were stained with fluorescent antibodies against vWF, which stains endothelial cells and factor VIII released by permeable vessels and αSMA which is found in pericytes lining mature blood vessels and in contractile myofibroblasts. Figure 15 shows representative images of sections of control and treated chronic limb wounds taken after 7 and 14 days. Equivalent images of vWF/SMA stained sections of body wounds are shown in Appendix 1, Supplementary Figure 2. After 7 days, a large amount of vWF staining was observed at the new granulation tissue of both chronic and body wounds and a further increase was observed after 14 days (Fig. 15, Sup. Fig. 2). At 7 days, vWF staining appeared to be greater in treated wounds than in both the chronic and body control wounds, (Fig. 15, Sup. Fig. 2). A large amount of αSMA staining was also observed in the wounds, which increased between 7 and 14 days (Fig. 15, Sup. Fig. 2), although the levels were more variable in the limb wounds. Although an increase in αSMA staining was observed in treated limb wounds at day 7, there appeared to be less staining in the treated limb and body wounds than the controls by day 14 (Fig. 15, Sup. Fig. 2).

Closer examination of the stained sections showed that, at day 7 and 14, mature blood vessels, in which vWF^{+ve} endothelial cells were lined by αSMA^{+ve} pericytes (Fig. 16A), were present in the granulation tissue of both control and treated wounds. At day 7, however, there was a large amount of vWF staining that was not associated with nuclei (Fig. 16B), which indicates factor VIII release from leaky vessels. This was particularly evident in the treated limb sections. At day 7 and day 14, αSMA^{+ve}

myofibroblasts, that were not associated with vWF^{+ve} endothelial cells (Fig. 16C), were present in the granulation tissue of both control and treated wounds. These cells were most evident in the control limb sections and appeared to be reduced in number or intensity in body and treated wounds.

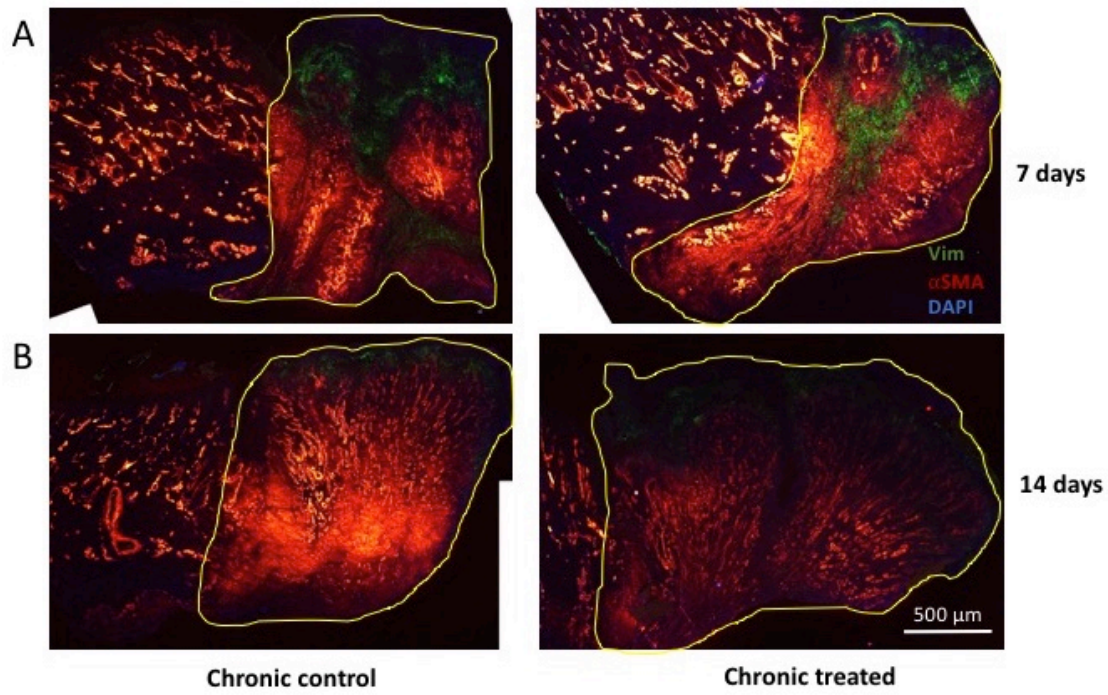

Figure 15. Re-vascularisation in chronic limb wounds in response to treatment with VEGF-E and vIL-10. Images of sections from treated and control chronic limb wounds from (A) 7 days and (B) 14 days, stained with antibodies against vWF (marker of endothelial cells and factor VIII), αSMA (marker of pericytes and myofibroblasts) and DAPI (nuclear stain). ImageJ software was used to determine the percentage of the granulation tissue area stained with each antibody (outlines in yellow). Scale indicated.

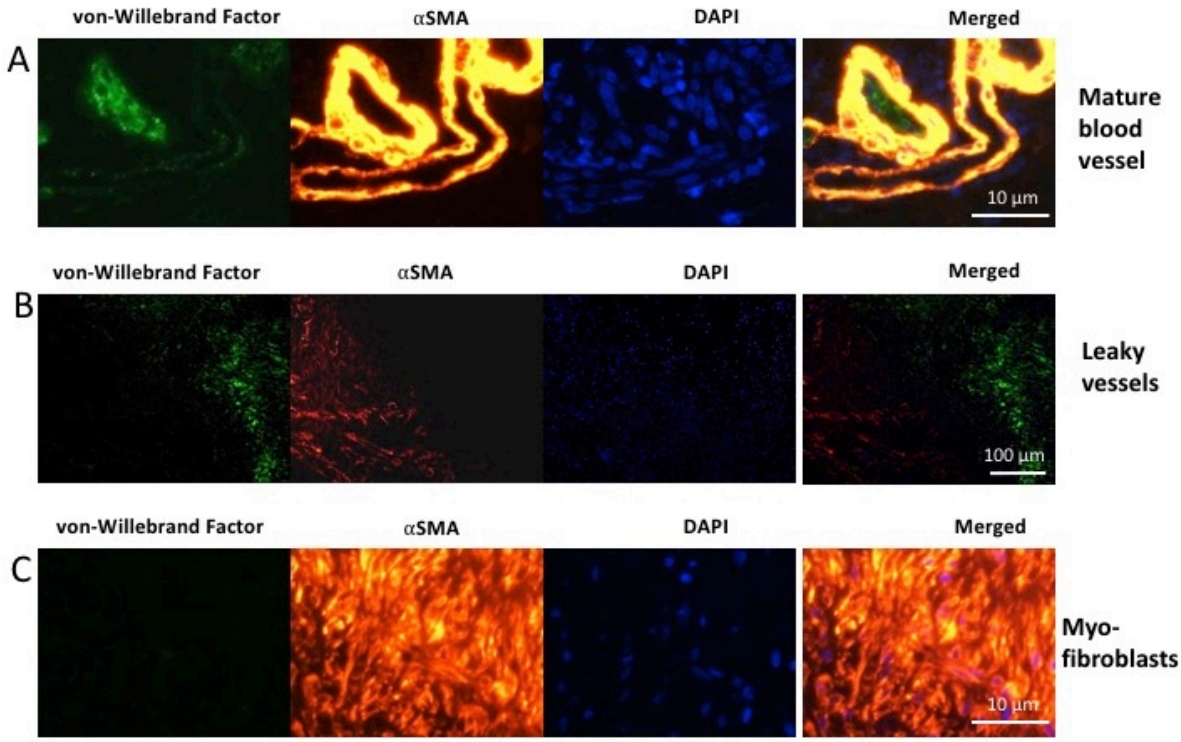

Figure 16. Specific staining of features in equine wounds shown by staining with vWF and αSMA. Images showing (A) $\alpha SMA^{+}/vWF^{+}$ mature blood vessels in a control body wound at 7 days, (B) $\alpha SMA^{-}/vWF^{+}$ staining of Factor VIII indicating edema in a control chronic wound at 7 days and (C) $\alpha SMA^{+}/vWF^{-}$ myofibroblasts in a control chronic wound at 14 days. Individual and merged images are shown. Scale is indicated.

Image J was then used to analyse the gross changes in vWF and αSMA staining in the granulation tissue of body and chronic limb wounds between those treated with VEGF-E and vIL-10 and the controls. The percentage area of granulation tissue stained with vWF increased from day 7 to day 14 in both body and limb wounds (Fig. 17A-B). There was a trend towards increased staining of vWF in the treated wounds compared to the control wounds at 7 days (Fig. 17A-B), but no differences were observed after 14 days. The percentage area of αSMA staining also increased from day 7 to day 14 in both body and limb wounds (Fig. 17C-D). There was a slight increase in staining of αSMA in the treated limb wounds compared to the control wounds at 7 days, but by 14

days there was a slight reduction in the treated body and limb wounds compared with the matched controls.

These results indicate that treatment with the VEGF-E and vIL-10 may have influenced blood vessel and myofibroblast formation in the equine wounds but more detailed analyses are needed to differentiate the contribution of the different cell types.

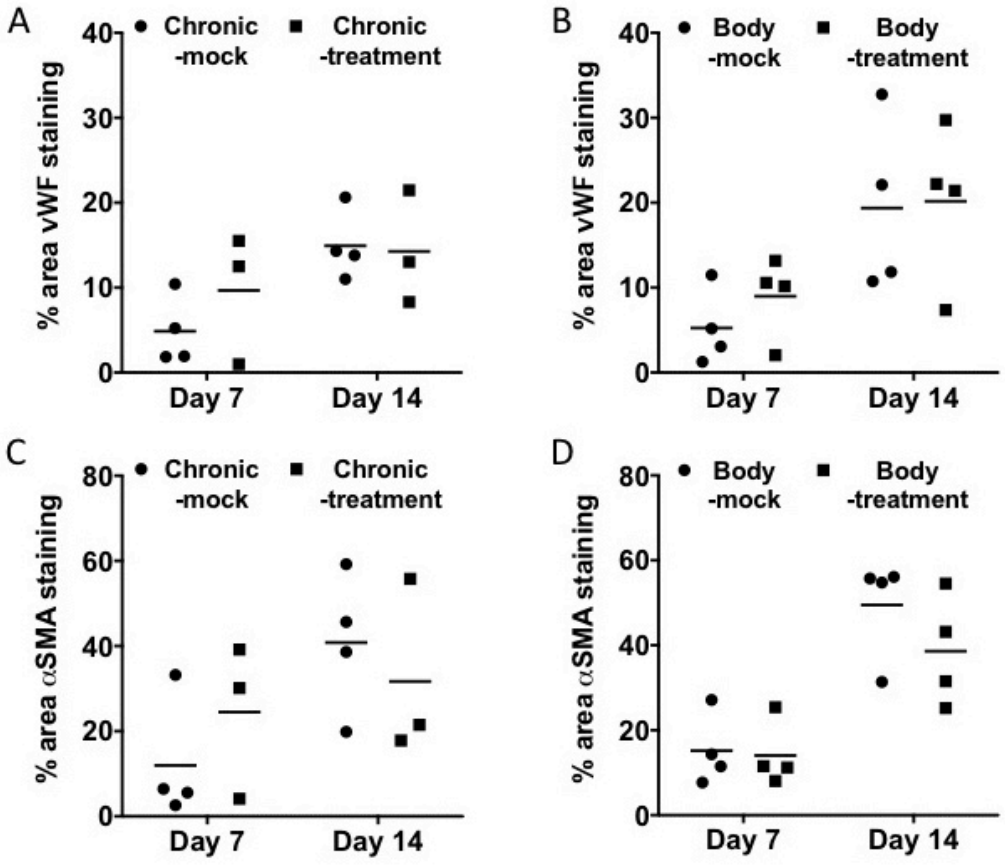

Figure 17. Quantification of re-vascularisation in equine wounds in response to treatment with VEGF-E and vIL-10. Image J software was used to measure the percentage of granulation tissue area stained with (A-B) vWF or (C-D) αSMA in sections from (A, C) chronic and (B, D) body wounds. Values represent mean ± SEM (n = 3-4). An unpaired *t*-test was used to identify significant differences between control and treated horses at each time point and no *P* values ≤0.1 were obtained.

3.2.4 Effects of the viral proteins on innate immune cell trafficking in equine skin wounds

In order to assess the effects of the viral treatment on the immune cell content, zinc-fixed paraffin-embedded sections of biopsies taken from the limb and body wounds at day 7 were stained with fluorescent antibodies against major histocompatibility complex class II (MHC-II), which stains dendritic cells, monocytes and macrophages. Figure 18 shows a representative image of a section from control and treated chronic limb wounds. Equivalent images of MHC-II stained sections of body wounds are shown in Appendix 1, Supplementary Figure 4. At 7 days, a small amount of MHC-II staining was observed at the edge of the granulation tissue and scattered throughout the adjacent tissue (Fig. 18A-B, Sup. Fig. 4A-B). Closer examination showed the staining was specific for nucleated cells (Fig. 18C). A decrease in the number of cells stained with MHC-II was also evident in the chronic limb wounds treated with the VEGF-E and vIL-10 when compared with control wounds (Fig. 18A-B).

Image J was then used to analyse the overall change in MHC-II staining in the wound sections from body and chronic limb wounds between those treated with VEGF-E and vIL-10 and the controls. The percentage area of tissue stained with MHC-II at day 7 was variable but equivalent in the body and limb wounds (Fig. 19A-B). There was however a trend towards a decrease in MHC-II staining in the treated limb and body wounds compared to their controls (Fig. 19A-B, not significant and $P = 0.1$ respectively).

These results indicate that treatment with the VEGF-E and vIL-10 may have reduced the recruitment of innate immune cells into the equine wounds but more detailed analyses are needed to differentiate the contribution of the different cell types.

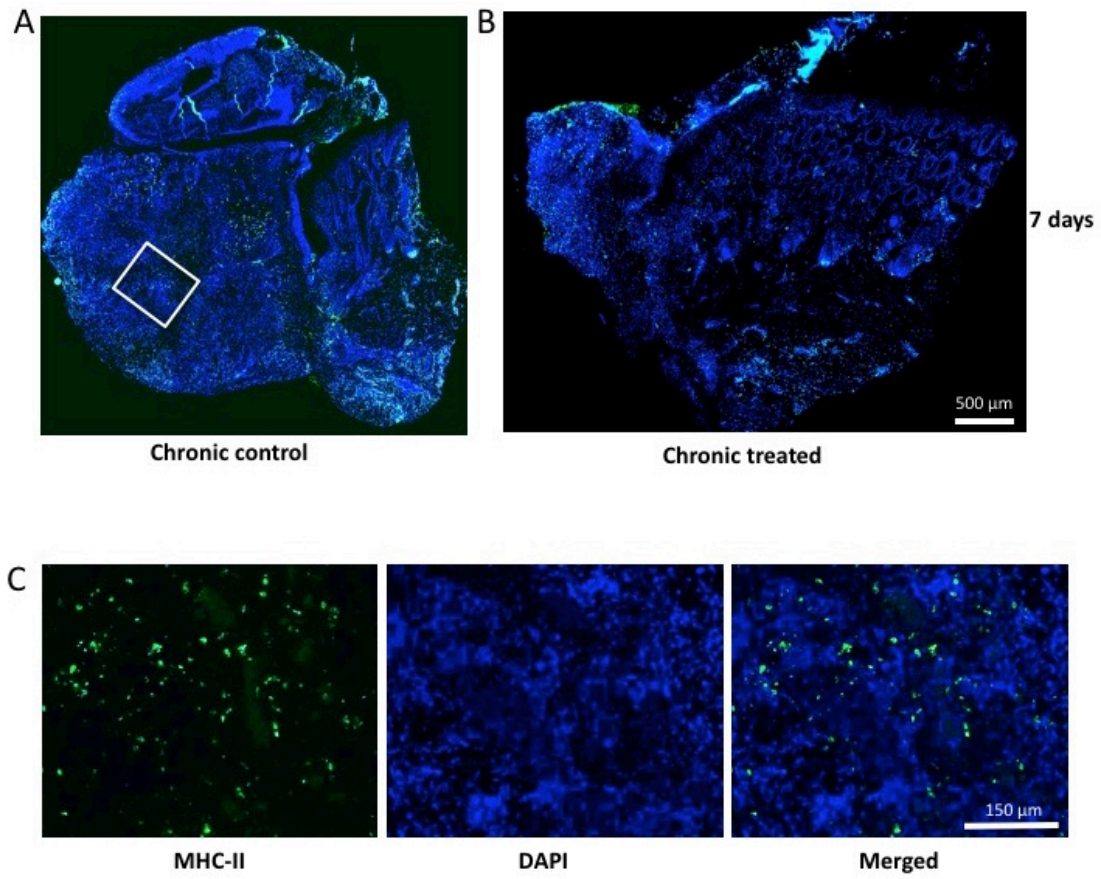

Figure 18. Immune cells in chronic limb wounds in response to treatment with VEGF-E and vIL-10. Images of sections from (A) control and (B) treated chronic wounds from 7 days stained with an antibody against MHC-II and DAPI (nuclear stain). (C) Images showing MHC-II specific staining in a control limb wound at 7 days. Individual and merged images are shown. Scale indicated.

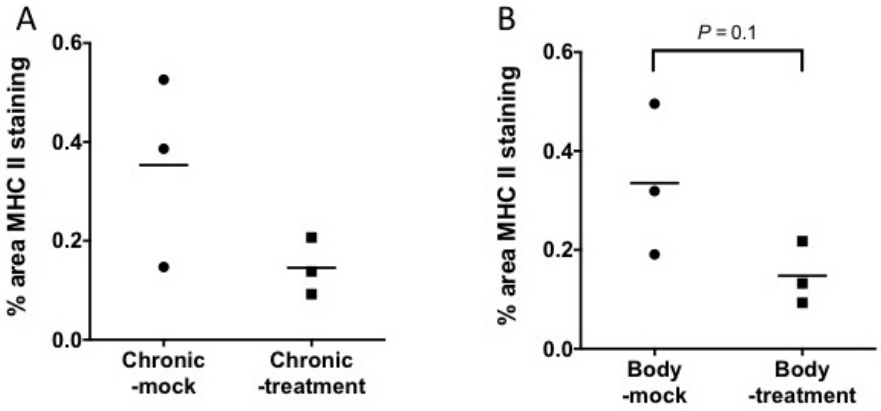

Figure 19. Quantification of innate immune cell content in equine wounds in response to treatment with VEGF-E and vIL-10. Image J software was used to measure the percentage of the section from (A) chronic and (B) body wounds stained with MHC-II. Values represent mean ± SEM (n = 3-4). Values represent mean ± SEM (n = 3). A paired *t*-test was used to identify significant differences between control and treated horses at each time point and *P* values ≤0.1 are indicated.

4 Discussion

VEGF-E and vIL-10 have previously been shown to improve skin repair by improving wound re-epithelisation, vascularisation and by limiting inflammation and fibrosis. This project aimed to determine the effect of the above-mentioned proteins in equine tissue. There were two objectives to this study; the first to determine if the viral proteins are effective on equine cells using an *in vitro* equine cell line, and second to determine if the proteins improved healing in horses in an *in vivo* trial of chronic equine wounds.

4.1 VEGF-E in equine systems

VEGF-E is a vascular endothelial growth factor, and has been previously reported to increase vascularisation and epidermal regeneration in murine wounds and in ovine skin (Savory *et al*., 2000; Wise *et al*., 2007; Wise *et al*., 2012; Wise *et al*., 2003). The cellular homolog, VEGF-A, has also been shown to increase human fibroblast proliferation (Zhao *et al*., 2013). VEGF-E has been shown to increase genes involved in inflammation in murine and human cells, as well as induce changes in expression of VEGF-A and the VEGF receptors (unpublished). These changes in VEGF expression are relative to the dosage of the VEGF-E; low levels of VEGF-E will upregulate the expression of cellular VEGF and its receptors, while too much VEGF-E will cause a negative-feedback loop resulting in a down regulation of cellular VEGF. Orf virus primarily infects sheep, and the ovine receptor for VEGF-E, VEGFR2, shares 84% amino acid homology with the murine equivalent. Equine VEGFR2 shares an even closer 94% homology to the ovine receptor, indicating that VEGF-E will actively bind the equine receptor.

An equine fibroblast cell line expressing eVEGFR2 was used to determine the effects of VEGF-E on proliferation, migration, and gene expression. The results of the scratch assay showed no changes in proliferation or migration in response to VEGF-E. The protein altered the expression of eIL-10 in the fibroblasts, but had no other effects on gene expression. These results indicate that VEGF-E is having virtually no effect on the fibroblasts. One potential hypothesis for this result is that VEGF-E is not a mitogen for equine fibroblasts. Another hypothesis could be that the effects of VEGFs in equine fibroblasts are not mediated through VEGFR2, but rather through either VEGFR1 or VEGFR3. This would suggest that VEGF-E may have the ability to work in other equine cells to promote proliferation. As VEGF-E has been previously shown to activate murine keratinocytes, the equine equivalent of these cells would be a more suitable cell line to use to observe the bioactivity of the viral proteins. Equine endothelial cells may also exhibit responses to VEGF-E.

Chronic wounds were developed in thoroughbred horses and treated with a combination of vIL-10 and VEGF-E, to determine the effectiveness of the viral proteins in improving wound repair. Skin samples were analysed for changes in histology and gene expression. An immediate increase in Factor VIII staining was seen for the treated samples, indicating an increase in edema. This was accompanied by swelling around the wound edge, as illustrated by images taken of the treated wound sites (Appendix 1, Supplementary Figure 3). These findings indicate VEGF-E treatment has induced an increase in vascular permeability. Gene expression analyses of chronic wounds showed that VEGF-A was down regulated in response to the proteins. This indicates that perhaps the concentration of VEGF-E administered was too high, resulting in a negative regulation of its cellular counterpart.

Skin samples were also stained against α-SMA to identify pericytes surrounding blood vessels. This staining was greater in treated samples at later time points, indicating that there are more mature blood vessels in response to the treatment. However, the integrity of these vessels is not known. This finding is concurrent with other publications which indicate that equine limb wound beds are highly vascularised, but vessels are occluded and so the wound lacks adequate levels of oxygen (Dubuc et al., 2006; Lepault et al., 2005). This project did not investigate the integrity of the blood vessels, and so further analysis would be required to determine if treatment with the viral proteins had any impact on their integrity. Histological analysis can be performed using transmission electron microscopy to examine the cross-section of blood vessels and measure the size of endothelial cells in order to determine if the lumen of the vessel is being occluded by oversized endothelial cells, as shown in previous studies.

VEGF-E has been shown to increase epidermal regeneration, and the results from the *in vivo* portion of this study concurred with these findings. However, gross analysis of the horse wounds found that there were no changes in overall wound closure (unpublished), and this suggests the epidermal regeneration observed in this study was only a transient response. This could indicate that the VEGF-E treatment is having an effect on the skin, but only for a short period of time. The treatment regime needs to extend over a longer period of time if it is to promote wound closure.

VEGFR2 expression significantly decreased in limb skin in the first 48 hours after wounding, during which time the treatment was applied. This could result in poor VEGF-E signalling, limiting the effects seen in response to the protein. VEGF-E dosage also requires further optimisation, as the immediate response in edema and swelling and the decrease in VEGF-A expression indicate that while the protein appears

to exert some effect on the skin, the concentration of VEGF-E in this treatment may have been too high.

4.2 Viral IL-10 in equine systems

Viral IL-10 has been shown to reduce inflammation and fibrosis in murine wounds to reduce scarring and enhance wound repair (Wise et al., 2014). Cellular IL-10 has also been shown to limit fibroblast migration and regulate collagen production through the induction of MMP-1 (Moroguchi et al., 2004; Yamamoto et al., 2001). Treatment with vIL-10 has previously been shown to reduce the expression of genes involved in inflammation and fibrosis, as well as limit fibroblast proliferation and prevent infiltration of immune cells (Wise et al., 2014).

The ovine receptor for IL-10, IL-10Rα, shares 53% amino acid homology with the murine equivalent. Equine IL-10Rα shares an even closer 65% homology to the ovine receptor, indicating that IL-10 will actively bind the equine receptor.

Equine fibroblasts showed no change in proliferation or migration when exposed to vIL-10. There was however an increase in the production of collagenase-1 and a reduction in the expression of anti-inflammatory genes. The changes in equine fibroblast gene expression in response to polyI:C showed varying effects, indicating that further optimisation of polyI:C concentration is needed. The treatment of equine fibroblasts with vIL-10 indicated that the protein may be having a small effect, but further optimisation of dosage and timing in the assays is required.

The treatment of chronic wounds in horses consisted of a combination of VEGF-E and vIL-10. It was expected that vIL-10 would down regulate the genes involved in inflammation and fibrosis and prevent inflammatory cell infiltration into the wound. The results of wound gene expression analyses showed a temporary reduction in inflammatory and fibrotic genes in response to the protein treatment, as

well as changes in anti-inflammatory genes. The reduction in IL-10 expression indicates a negative feedback loop preventing further production of IL-10. The receptor for IL-10 was upregulated in treated samples, indicating that the vIL-10 is promoting an increase in cell signalling. Viral IL-10 has also been shown to reduce fibrosis and prevent scarring (Wise et al., 2014). TGFβ_1 is a cytokine that stimulates fibroblasts to produce collagen. This study showed that viral protein treatment transiently reduced the expression of TGFβ_1 and Col3α1, which may reduce the amount of collagen produced and could limit scarring.

Treatment of murine wounds with vIL-10 was shown to reduce macrophage infiltration (Wise et al., 2014). Immunohistochemical staining of wound tissue showed a reduction in MHC-II$^+$ cells in treated skin after 7 days. This correlates with the reduction of inflammatory gene expression, indicating that vIL-10 is preventing the infiltration of innate immune cells such as monocytes and dendritic cells by reducing the production of inflammatory cytokines and chemokines.

Treatment of murine wounds with vIL-10 has previously been shown to reduce myofibroblast differentiation while increasing the association of pericytes with endothelial cells (Wise et al., 2014). Immunohistochemical staining against αSMA and vWF indicated an increase in the amount of blood vessels in treated samples. While the increase in the number of blood vessels is likely due to the effects of VEGF-E, the greater αSMA staining around the blood vessels after 14 days indicates an increase in pericyte coverage, which results in more stable vessels (von Tell et al., 2006). The overall reduction in αSMA staining in treated wounds may also indicate a reduction in myofibroblast differentiation.

The effects of the vIL-10 protein appeared to be transient and there were no long-term changes in wound closure or scarring (unpublished). Expression of the IL-

10Rα receptor decreased over time, and the low expression of this receptor may result in a reduction in responsiveness, and therefore less long-term effectiveness. The treatment was only administered within the first 72 hours after wounding, and led to increased expression of the IL-10 receptor; hence if the timing of the treatments were extended to a longer period of time, there may be more improved long-term wound resolution.

4.3 Limitations of VEGF-E and vIL-10 as an equine therapeutic

In summary, no clear effects of the viral proteins were observed using equine fibroblasts, and the effects seen in equine skin appeared to be transient and did not result in an improved wound closure rate. To obtain therapeutic benefits for chronic equine wounds the treatment regime would need further optimisation to establish a more effective concentration and dosing regime.

Changes were seen in the epidermal coverage of the wound in the 14-day period. This indicates that VEGF-E is having an effect on wound closure. However, this treatment was administered subcutaneously, and this could mean that the treatment is not having the desired chemotactic effect on the upper epidermal layer as it is administered too far from the site. For this reason, a topical application of VEGF-E directly onto the wound may exhibit greater epidermal closure over the wound healing period.

Osteopontin is expressed on inflammatory cells such as macrophages, and the expression of this gene was reduced in the wounded equine skin, indicating that there is a lack of macrophages in the wound during repair and resolution. Macrophages release cytokines such as VEGF which promotes angiogenesis and TGFβ_1 and PDGF to promote vessel stabilisation (Wynn and Barron, 2010). Treatment of a reduced dose of

VEGF-E, or even equine VEGF-A early in the wounding process would result in a low level of sustained inflammation to allow the infiltration of innate immune cells, including macrophages. This would stimulate a small inflammatory response that would promote blood vessel formation. Viral or equine IL-10 introduced later in the treatment could then act to dampen these responses to prevent the extended inflammatory response and the development of excessive fibrosis, thus allowing the wound to close effectively while reducing scar formation.

VEGF-E increased the production of blood vessels, but this was accompanied with an increase in Factor VIII staining, indicating that the vessels were permeable. PDGF or angiopoietin-1 can increase the maturation and integrity of blood vessels by recruiting pericytes to the vessels (Bergers and Song, 2005; Heldin and Westermark, 1999; Moss, 2013). The expression of PDGFβ_1 was significantly reduced in wounded skin. PDGFβ or Ang1 could be added early in the treatment regime to increase levels and thereby help to stabilise new blood vessels and improve functionality. Alternatively, the anti-angiogenic molecules SPARC, THBS2 or PEPF, which are also under expressed in equine limb wounds could be concurrently administered with VEGF-E to improve vessel function (Theoret and Wilmink, 2013).

4.4 Concluding remarks

The aim of this preliminary study was to determine if vIL-10 and VEGF-E would act on equine cells. An equine fibroblast cell line was generated, and the proteins had little effect on migration and minor effects on the expression of inflammatory and fibrotic genes. The proteins did have an effect in chronic limb wounds, altering expression of inflammatory and fibrotic genes and increasing wound re-vascularisation and epidermal regeneration, while limiting innate immune cell recruitment. However, these results were transient and there was no overall change in the rate of wound

closure. Therefore, further optimisation is required if these proteins were to be pursued as a potential therapeutic for chronic equine wounds.

5 References

Barrientos, S., Stojadinovic, O., Golinko, M.S., Brem, H., and Tomic-Canic, M. (2008). Growth factors and cytokines in wound healing. Wound Repair Regen *16*, 585-601.

Beck, L.S., Deguzman, L., Lee, W.P., Xu, Y., McFatridge, L.A., and Amento, E.P. (1991). TGF-β1 Accelerates Wound Healing: Reversal of Steroid-Impaired Healing in Rats and Rabbits. Growth Factors *5*, 295-304.

Bello, T.R. (2002). Practical treatment of body and open leg wounds of horses with bovine collagen, biosynthetic wound dressing and cyanoacrylate. Journal of Equine Veterinary Science *22*, 157-164.

Bergers, G., and Song, S. (2005). The role of pericytes in blood-vessel formation and maintenance. Neuro-oncology *7*, 452-464.

Berry, D.B., and Sullins, K.E. (2003). Effects of topical application of antimicrobials and bandaging on healing and granulation tissue formation in wounds of the distal aspect of the limbs in horses. American Journal of Veterinary Research *64*, 88-92.

Bischofberger, A.S., Dart, C.M., Perkins, N.R., and Dart, A.J. (2011). A preliminary study on the effect of manuka honey on second-intention healing of contaminated wounds on the distal aspect of the forelimbs of horses. Vet Surg *40*, 898-902.

Bischofberger, A.S., Tsang, A.S., Horadagoda, N., Dart, C.M., Perkins, N.R., Jeffcott, L.B., Jackson, C.J., and Dart, A.J. (2015). Effect of activated protein C in second intention healing of equine distal limb wounds: a preliminary study. Australian veterinary journal *93*, 361-366.

Braddock, M., Campbell, C.J., and Zuder, D. (1999). Current therapies for wound healing - electrical stimulation, biological therapeutics and the potential for gene therapy. International Journal of Dermatology *38*, 808-817.

Brown, G.L., Nanney, L.B., Griffen, J., Cramer, A.B., Yancey, J.M., Curtsinger, L.J., Holtzin, L., Schultz, G.S., Jurkiewicz, M.J., and Lynch, J.B. (1989). Enhancement of wound healing by topical treatment with epidermal growth factor. The New England Journal of Medicine *321*, 76-79.

Bussche, L., Harman, R.M., Syracuse, B.A., Plante, E.L., Lu, Y.C., Curtis, T.M., Ma, M., and Van de Walle, G.R. (2015). Microencapsulated equine mesenchymal stromal cells promote cutaneous wound healing in vitro. Stem cell research & therapy *6*, 66.

Demidova-Rice, T.N., Hamblin, M.R., and Herman, I.M. (2012). Acute and impaired wound healing: pathophysiology and current methods for drug delivery, part 1: normal and chronic wounds: biology, causes, and approaches to care. Advanced Skin Wound Care *25*, 304-314.

Dubuc, V., Lepault, E., and Theoret, C.L. (2006). Endothelial cell hypertrophy is associated with microvascular occlusion in horse wounds. Canadian Journal of Veterinary Research *70*, 206-210.

Engelen, M., Besche, B., Lefay, M., Hare, J., and Vlaminck, K. (2004). Effects of ketanserin on hypergranulation tissue formation, infection and helaing of equine lower limb wounds. Canadian Veterinary Journal *45*, 144-149.

Fleming, S.B., Wise, L.M., and Mercer, A.A. (2015). Molecular genetic analysis of orf virus: a poxvirus that has adapted to skin. Viruses *7*, 1505-1539.

Galiano, R.D., Tepper, O.M., Pelo, C.R., Bhatt, K.A., Callaghan, M., Bastidas, N., Bunting, S., Steinmetz, H.G., and Gurtner, G.C. (2004). Topical vascular endothelial growth factor accelerates diabetic wound healing through increased angiogenesis and by mobilizing and recruiting bone marrow-derived cells. American Journal of Pathology *164*, 1935-1947.

Gurtner, G.C., Werner, S., Barrandon, Y., and Longaker, M.T. (2008). Wound repair and regeneration. Nature *453*, 314-321.

Hamidi, S., Schafer-Korting, M., and Weindl, G. (2014). TLR2/1 and sphingosine 1-phosphate modulate inflammation, myofibroblast differentiation and cell migration in fibroblasts. Biochimica et biophysica acta *1841*, 484-494.

Heldin, C., and Westermark, B. (1999). Mechanism of action and in vivo role of platelet-derived growth factor. Physiological Reviews *79*, 1283-1316.

Holmes, K., Roberts, O.L., Thomas, A.M., and Cross, M.J. (2007). Vascular endothelial growth factor receptor-2: structure, function, intracellular signalling and therapeutic inhibition. Cellular signalling *19*, 2003-2012.

Hulkower, K.I., and Herber, R.L. (2011). Cell migration and invasion assays as tools for drug discovery. Pharmaceutics *3*, 107-124.

Imlach, W., McCaughan, C.A., Mercer, A.A., Haig, D., and Fleming, S.B. (2002). Orf-virus interleukin-10 stimulates the proliferation of murine mast cells and inhibits cytokine synthesis in murine peritoneal macrophages. Journal of General Virology *83*, 1049-1058.

Johnson, K.E., and Wilgus, T.A. (2014). Vascular Endothelial Growth Factor and Angiogenesis in the Regulation of Cutaneous Wound Repair. Advances in wound care *3*, 647-661.

Lai-Cheong, J.E., and McGrath, J.A. (2009). Structure and Function of Skin, Hair and Nails. Medicine *35*, 223-226.

Leibovich, S.J., and Ross, R. (1975). The Role of Macrophage in Wound Repair. American Journal of Pathology *78*, 71-92.

Lepault, E., Celeste, C., Dore, M., Martineau, D., and Theoret, C.L. (2005). Comparative study on microvascular occlusion and apoptosis in body and limb wounds in the horse. Wound Repair and Regeneration *13*, 520-529.

Martin, P. (1997). Wound Healing - Aiming for perfect skin regeneration. Science *276*, 75-81.

Mercer, A.A., Ueda, N., Friederichs, S.M., Hofmann, K., Fraser, K.M., Bateman, T., and Fleming, S.B. (2006). Comparative analysis of genome sequences of three isolates of Orf virus reveals unexpected sequence variation. Virus Research *116*, 146-158.

Moroguchi, A., Ishimura, K., Okano, K., Wakabayashi, H., Maeba, T., and Maeta, H. (2004). Interleukin-10 suppresses proliferation and remodeling of extracellular matrix of cultured human skin fibroblasts. European surgical research Europaische chirurgische Forschung Recherches chirurgicales europeennes *36*, 39-44.

Moss, A. (2013). The angiopoietin:Tie 2 interaction: a potential target for future therapies in human vascular disease. Cytokine & growth factor reviews *24*, 579-592.

Nall, A.V., Brownlee, R.E., Colvin, P., Schultz, G., Fein, D., Cassisi, N.J., Nguyen, T., and Kalra, A. (1996). Transforming growth facter β1 improves wound healing and random flap survival in normal and irradiated rats. Archives of Otolaryngology - Head and Neck Surgery *122*, 171-177.

Ono, I., Akasaka, Y., Kikuchi, R., Sakemoto, A., Kamiya, T., Yamashita, T., and Jimbow, K. (2007). Basic fibroblast growth factor reduces scar formation in acute incisional wounds. Wound Repair and Regeneration *15*, 617-623.

Ono, I., Yamashita, T., Hida, T., Jin, H.Y., Ito, Y., Hamada, H., Akasaka, Y., Ishii, T., and Jimbow, K. (2004). Local administration of hepatocyte growth factor gene enhances the regeneration of dermis in acute incisional wounds. The Journal of surgical research *120*, 47-55.

Rennert, R.C., Rodrigues, M., Wong, V.W., Duscher, D., Hu, M., Maan, Z., Sorkin, M., Gurtner, G.C., and Longaker, M.T. (2013). Biological therapies for the treatment of cutaneous wounds: phase III and launched therapies. Expert Opinion on Biolgical Therapy *13*, 1523-1541.

Rose, M.T. (2012). Effect of growth factors on the migration of equine oral and limb fibroblasts using an in vitro scratch assay. Veterinary journal *193*, 539-544.

Russell, S.B., Russell, J.D., Trupin, K.M., Gayden, A.E., Opalenik, S.R., Nanney, L.B., Broquist, A.H., Raju, L., and Williams, S.M. (2010). Epigenetically altered wound healing in keloid fibroblasts. The Journal of investigative dermatology *130*, 2489-2496.

Sato, Y., Ohshima, T., and Kondo, T. (1999). Regulatory role of endogenous interleukin-10 in cutaneous inflammatory response of murine wound healing. Biochemical and biophysical research communications *265*, 194-199.

Savory, L.J., Stacker, S.A., Fleming, S.B., Niven, B.E., and Mercer, A.A. (2000). Viral vascular endothelial growth factor plays a critical role in orf virus infection. Journal of Virology *74*, 10699-10706.

Sen, C.K., Gordillo, G.M., Roy, S., Kirsner, R., Lambert, L., Hunt, T.K., Gottrup, F., Gurtner, G.C., and Longaker, M.T. (2009). Human skin wounds: a major and snowballing threat to public health and the economy. Wound Repair Regen *17*, 763-771.

Shaw, T.J., and Martin, P. (2009). Wound repair at a glance. Journal of Cell Science *122*, 3209-3213.

Sherman, R.A., Morrison, S., and Ng, D. (2007). Maggot debridement therapy for serious horse wounds - a survey of practitioners. The Veterinary Journal *174*, 86-91.

Shibuya, M. (2006). Vascular endothelial growth factor receptor-1 (VEGFR-1/Flt-1): a dual regulator for angiogenesis. Angiogenesis *9*, 225-230; discussion 231.

Theoret, C. (2009). Tissue engineering in wound repair: the three "R"s--repair, replace, regenerate. Veterinary Surgery *38*, 905-913.

Theoret, C.L., Barber, S.M., Moyana, T.N., and Gordon, J.R. (2001). Expression of transforming growth factor [beta], [beta], and basic fibroblast growth factor in full-thickness skin wounds of equine limbs and thorax. Veterinary Surgery *30*, 269-277.

Theoret, C.L., Barber, S.M., Moyana, T.N., and Gordon, J.R. (2002). Preliminary observations on expression of transforming growth factors [beta]1 and [beta]3 in equine full-thickness skin wounds healing normally or with exuberant granulation tissue. Veterinary Surgery *31*, 266-273.

Theoret, C.L., Olutoye, O.O., Parnell, L.K., and Hicks, J. (2013). Equine exuberant granulation tissue and human keloids: a comparative histopathologic study. Veterinary Surgery *42*, 783-789.

Theoret, C.L., and Wilmink, J.M. (2013). Aberrant wound healing in the horse: naturally occurring conditions reminiscent of those observed in man. Wound Repair and Regeneration *21*, 365-371.

Tracey, A.K., Alcott, C.J., Schleining, J.A., Safayi, S., Zaback, P.C., Hostetter, J.M., and Reinertson, E.L. (2014). The effects of topical oxygen therapy on equine distal limb dermal wound healing. Canadian Veterinary Journal *55*, 1146-1152.

Ud-Din, S., Volk, S.W., and Bayat, A. (2014). Regenerative healing, scar-free healing and scar formation across the species: current concepts and future perspectives. Experimental dermatology *23*, 615-619.

van den Boom, R., Wilmink, J.M., O'Kane, S., Wood, J., and Ferguson, M.W.J. (2002). Transforming growth factor-β levels during second-intention healing are related to the different course of wound contraction in horses and ponies. Wound Repair and Regeneration, 3.

Vangipuram, M., Ting, D., Kim, S., Diaz, R., and Schule, B. (2013). Skin punch biopsy explant culture for derivation of primary human fibroblasts. Journal of Visualized Experiments, e3779.

Viera, M.H., Amini, S., Valins, W., and Berman, B. (2010). Innovative therapies in the treatment of keloids and hypertrophic scars. Journal of Clinical and Aesthetic Dermatology *3*.

Volk, S.W., and Bohling, M.W. (2013). Comparative wound healing--are the small animal veterinarian's clinical patients an improved translational model for human wound healing research? Wound Repair Regen *21*, 372-381.

von Tell, D., Armulik, A., and Betsholtz, C. (2006). Pericytes and vascular stability. Exp Cell Res *312*, 623-629.

Westgate, S.J., Percival, S.V., Knottenbelt, D.C., Clegg, P.D., and Cochrane, C.A. (2010). Chronic equine wounds: What is the role of infection and biofilms? Veterinary Wounds *22*, 138-145.

Wickett, R.R., and Visscher, M.O. (2006). Structure and function of the epidermal barrier. American Journal of Infection Control *34*, S98-S110.

Wilmink, J.M., Stolk, P.W.T., Van Weeren, P.R., and Barneveld, A. (1999a). Differences in second-intention wound healing between horses and ponies: macroscopic aspects. Equine Veterinary Journal *31*, 53-60.

Wilmink, J.M., and van Weeren, P.R. (2004). Differences in wound healing between horses and ponies: Application of research results to the clinical approach of equine wounds. Clinical Techniques in Equine Practice *3*, 123-133.

Wilmink, J.M., Van Weeren, P.R., Stolk, P.W.T., Van Mil, F.N., and Barneveld, A. (1999b). Differences in second-intention wound healing between horses and ponies: histological aspects. Equine Veterinary Journal *31*, 61-67.

Wise, L., McCaughan, C., Tan, C.K., Mercer, A.A., and Fleming, S.B. (2007). Orf virus interleukin-10 inhibits cytokine synthesis in activated human THP-1 monocytes, but only partially impairs their proliferation. The Journal of general virology *88*, 1677-1682.

Wise, L.M., Inder, M.K., Real, N.C., Stuart, G.S., Fleming, S.B., and Mercer, A.A. (2012). The vascular endothelial growth factor (VEGF)-E encoded by orf virus regulates keratinocyte proliferation and migration and promotes epidermal regeneration. Cellular microbiology *14*, 1376-1390.

Wise, L.M., Stuart, G.S., Real, N.C., Fleming, S.B., and Mercer, A.A. (2014). Orf virus IL-10 accelerates wound healing while limiting inflammation and scarring. Wound Repair Regen *22*, 356-367.

Wise, L.M., Ueda, N., Dryden, N.H., Fleming, S.B., Caesar, C., Roufail, S., Achen, M.G., Stacker, S.A., and Mercer, A.A. (2003). Viral vascular endothelial growth factors vary extensively in amino acid sequence, receptor-binding specificities,

and the ability to induce vascular permeability yet are uniformly active mitogens. The Journal of biological chemistry *278*, 38004-38014.

Wise, L.M., Veikkola, T., Mercer, A.A., Savory, L.J., Fleming, S.B., Caesar, C., Vitali, A., Makinen, T., Alitalo, K., and Stacker, S.A. (1999). Vascular endothelial growth factor (VEGF)-like protein from orf virus NZ2 binds to VEGFR2 and neuropilin-1. Proceedings of the National Academy of Science *96*, 3071-3076.

Wynn, T.A., and Barron, L. (2010). Macrophages: master regulators of inflammation and fibrosis. Seminars in liver disease *30*, 245-257.

Yamada, S.S. (2003). Preparation of human epidermal keratinocyte cultures. Current Protocols in Cell Biology, 2.6.1-2.6.5.

Yamamoto, T., Eckes, B., and Krieg, T. (2001). Effect of interleukin-10 on the gene expression of type I collagen, fibronectin, and decorin in human skin fibroblasts: differential regulation by transforming growth factor-beta and monocyte chemoattractant protein-1. Biochemical and biophysical research communications *281*, 200-205.

Yung, A. (2014). The structure of normal skin (DermNet NZ: Waikato Disrict Health Board).

Zhao, J., Hu, L., Liu, J., Gong, N., and Chen, L. (2013). The effects of cytokines in adipose stem cell-conditioned medium on the migration and proliferation of skin fibroblasts in vitro. BioMed research international *2013*, 578479.

Zhao, T., Zhao, W., Meng, W., Liu, C., Chen, Y., and Sun, Y. (2014). Vascular endothelial growth factor-C: its unrevealed role in fibrogenesis. American journal of physiology Heart and circulatory physiology *306*, H789-796.

6 Appendix 1

Supplementary Table 1. Primers used in this study. Table outlining primer names, accession numbers, sequences, product sizes and efficiencies.

Gene name	Accession no	Reference	Primer name	Primer sequence	Size	% efficiencies
eGAPDH	NM_001163856.1	Taylor et al 2009	eGAPDH F1	GCATCGTGGAGGGACTCA	84	105.35
			eGAPDH R1	GCCACATCTTCCCAGAGG		
eTNF-α	NM_001081819.1	Sanchez-Matamoros et al 2013	eTNF-a F2	TTACCGAATGCCTTCCAGTC	85	114.35
			eTNF-a R2	GGGCTACAGGCTTGTCACTT		
eVEGF-A	NM_001081821.1	Desnene et al 2012 F primer	eVEGF-A F1	CAACGACGAGGGCCTAGAGT	94	134.62
		changes to R primer	eVEGF-A R1	TCCTATGTGTTGGCTTTGGTGAGGT		
eCol1α2	XM_001492939.2	Taylor et al 2009	eCol1a2 F1	GCACATGCCGTGACTTGAGA	87	99.66
			eCol1a2 R1	CATCCATAGTGCATCCTTGATTAGG		
eCol3α1	XM_001917620.3	Taylor et al 2009	eCol3a1 F1	ACGCAAGGCCGTGAGACTA	63	105.25
			eCol3a1 R1	TGATCAGGACCACCAACATCA		
eMCP-1	NM_001081931.2	seq builder	eMCP-1 F1	GACCATATTGGCCAAGGAGATCTGTG	98	87.72
			eMCP-1 R1	AAGGCTTTGGAGTTTGGGCTTTC		
eMIP-2α	NM_001143955.1	seq builder	eMIP-2a F1	ATAGCCACTCTCAAGAATGGACAGGA	102	107.71
			eMIP-2a R1	TCAGTCGGAGCTGCCCTTGTTTA		
eαSMA	XM_001503035.4	seq builder	eaSMA F2	TCCGGGGGCACCACCAT	135	93.43
			eaSMA R2	GGAGCCGCCAATCCAGACAG		
eTGFβ1	NM_001081849.1	seq builder	eTGFb1 F1	GCAGAGCTGCGCCTCCTAAGG	96	92.71
			eTGFb1 R1	GTTACTGAGGTAGCGCCAGGAATTATTG		

eTGFβ3	XM_001492687.4	seq builder	eTGFb3 F1 eTGFb3 R1	CCATAAGTTCGACATGATCCAGGGC CACTGAGGACACGTTGAAGCGG	103	90.94
eIL-10	NM_001082490.1	seq builder	eIL-10 F3 eIl-10 R3	CAAGGCAGTGGAGCAGGTGAAGA CTTCGTTGTCATATAGGCTTCTATGTAGTTGAT	118	117.12
eCTGF	XM_001503316.3	seq builder	eCTGF F1 eCTGF R1	GCCTTGCGAAGCTGACCTGG CTCGAACTTGACAGGCTTGGAGATTT	88	95.63
eVEGF-R1	XM_003363176.2	seq builder	eVEGF-R1 F3 eVEGF-R1 R3	CTTTCACCAGATGCCCCTTCCAT AGGCCTTGGGTTTGCTCTCAGTC	112	123.07
eSPP-1	XM_001496152.2	seq builder	eSPP-1 F3 eSPP-1 R3	CCGTGATTTGCTTATGCCTCTTAGG CTTGAGCCATATGCTTACAGCATCTGA	125	106.76
eVEGF-R2	XM_00191694.3	seq builder	eVEGF-R2 F2 eVEGF-R2 R2	CAGTTGGGCTAAATGAGAGTTCCTTGTG GCCAGAGCTCATCATTTCCTTCCT	114	100.92
eFPR2	XM_005596470.1	seq builder	eFPR2 F2 eFPR2 R2	GAAGAGGAAGATAACCGTCACTGTGTTG TGGCAGCAATGAGGCCATAGC	113	85.65
eMMP-1	NM_001081847.2	seq builder	eMMP-1 F3 eMMP-1 R3	CAAATGGACTTCAAGCTGCTTATGAGG TATCCGTAGAGCACATCCTGCCC	106	87.72
PDGFβ	XM_005606646.1	seq builder	ePDGFβ F2 ePDGFβ R2	CGAGCCGGACAGCTTATCCC AGATCTCGAACACCTCGGTGCG	107	91.64
IL-10Rα	XM_001917543.2	seq builder	eIL-10Rα F2 eIL-10Rα R2	GGCGGTCTCCTGGGCACAT CCTCAGCCCAAGTCACTCAATCG	87	91.64

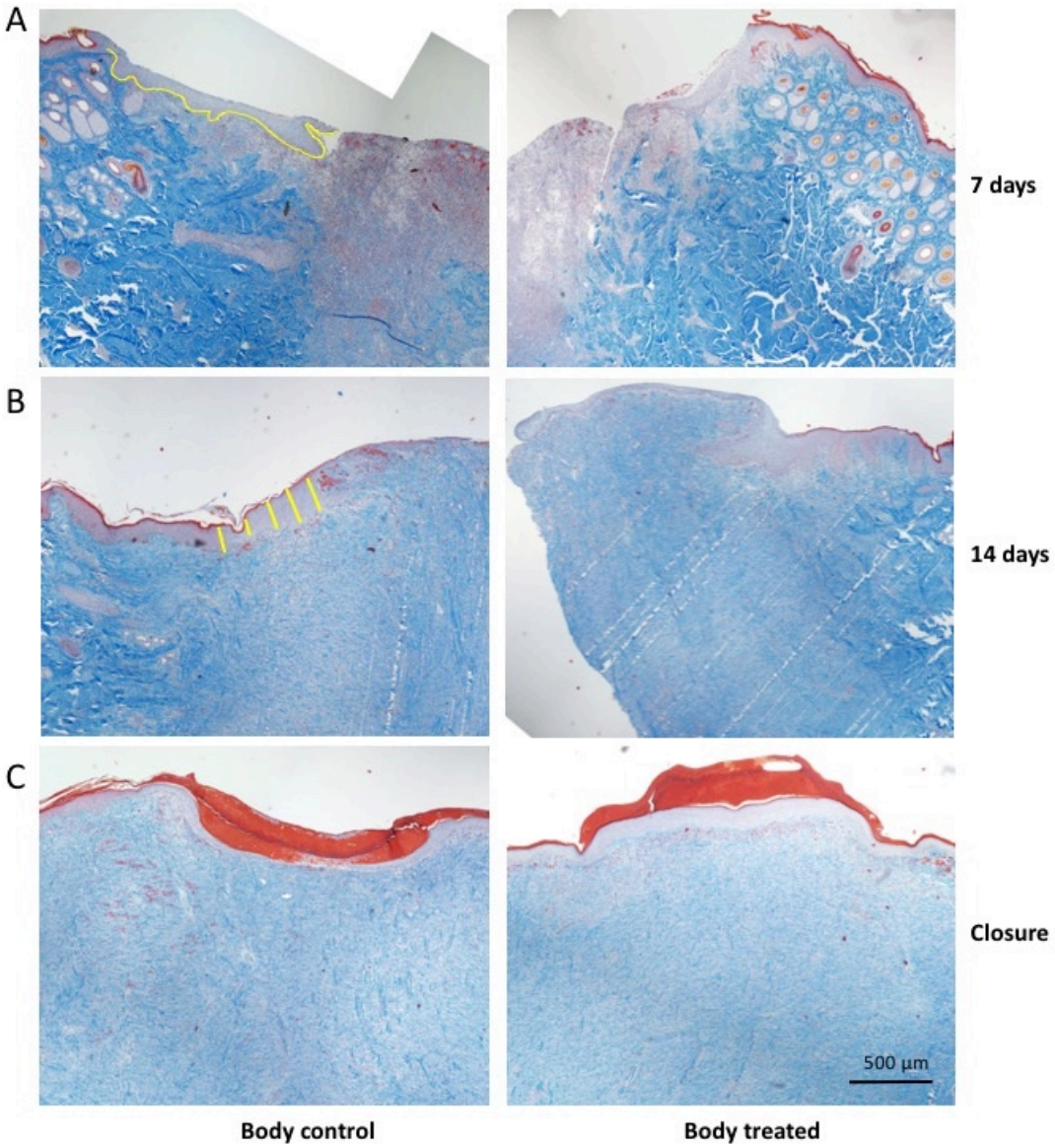

Supplementary Figure 1. Epidermal repair in body wounds in response to treatment with VEGF-E and vIL-10. Images of MSB-stained sections from treated and control body wounds harvested at (A) 7 days, (B) 14 days and (C) at final wound closure. Fibrin is stained red and collagen stained blue. ImageJ software was used to measure the length (contoured yellow line illustrated in (A)) and thickness (five yellow lines; thickness calculated as mean length of five lines illustrated in (B)) in the newly regenerating epidermis. Scale is indicated.

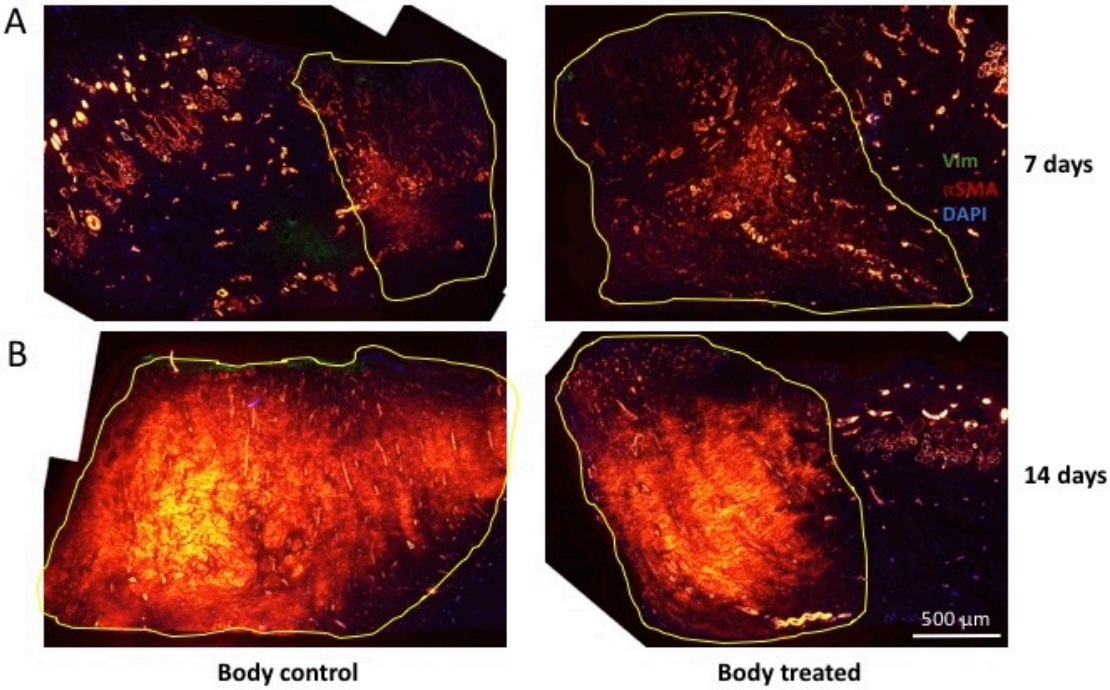

Supplementary Figure 2. Re-vascularisation in chronic limb wounds in response to treatment with VEGF-E and vIL-10. Images of sections from treated and control chronic limb wounds from (A) 7 days and (B) 14 days, stained with antibodies against vWF (marker of endothelial cells and factor VIII), αSMA (marker of pericytes and myofibroblasts) and DAPI (nuclear stain). ImageJ software was used to determine the percentage of the granulation tissue area stained with each antibody (outlines in yellow). Scale indicated.

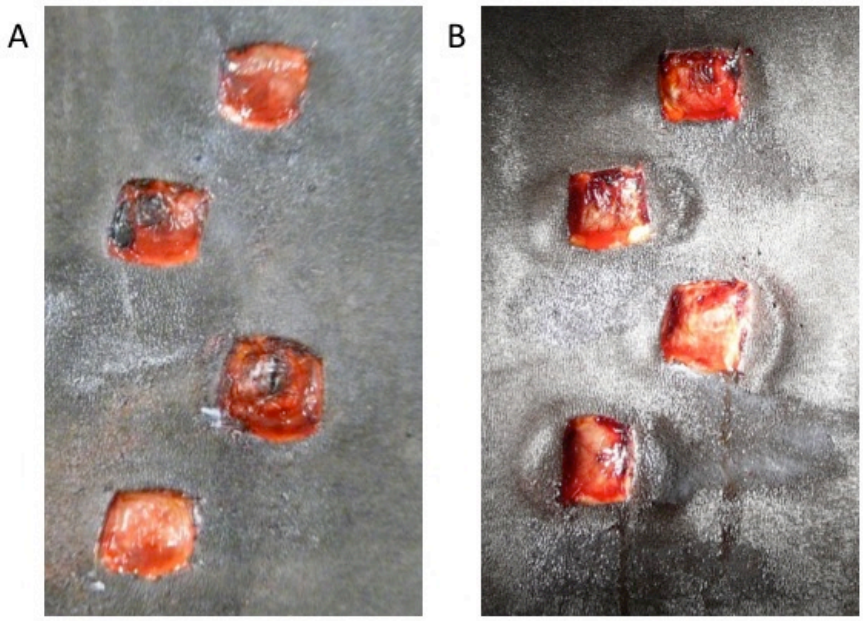

Supplementary Figure 3. Skin reaction to PBS or protein treatment. Images showing a flare response in equine skin wounds treated with (B) proteins (vIL-10 and VEGF-E), compared to (A) PBS treated control.

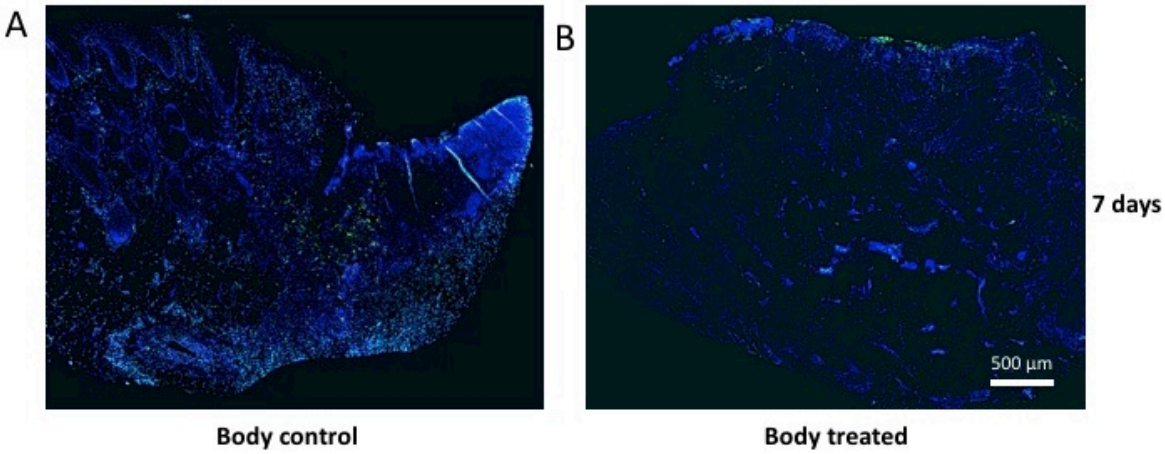

Supplementary Figure 4. Immune cells in body wounds in response to treatment with VEGF-E and vIL-10. Images of sections from (A) control and (B) treated body wounds from 7 days stained with an antibody against MHC-II and DAPI (nuclear stain).